Stability of rolls in rotating magnetoconvection in a layer with no-slip electrically insulating horizontal boundaries

Olga Podvigina
International Institute of Earthquake Prediction Theory and Mathematical Geophysics, 84/32 Profsoyuznaya St., 117997 Moscow, Russian Federation
and CNRS, Laboratoire Cassiopée, Observatoire de la Côte d'Azur BP 4229, 06304 Nice Cedex 4, France
(Received 1 December 2009; published 27 May 2010)

We consider the onset of Boussinesq convection in a horizontal layer of electrically conducting fluid rotating about a vertical axis with an imposed vertical magnetic field. Rigid electrically insulating horizontal boundaries are assumed. Our goal is to identify the region of parameter values, for which rolls emerge at the onset of convection. The following conditions are necessary for convective fluid motion to set in as stable rolls: instability of the trivial steady state is monotonic; the rolls bifurcate supercritically; they are stable to perturbations of the form of rolls rotated by any angle (without an imposed magnetic field this is called the Küppers-Lortz instability). For each of the three conditions we derive equations for respective boundaries in the parameter space and determine the boundaries numerically.

DOI: 10.1103/PhysRevE.81.056322 PACS number(s): 47.20.Bp, 47.65.−d, 47.10.Fg, 47.20.Ky

I. INTRODUCTION

We consider an electrically conducting fluid in a plane horizontal layer heated from below, rotating about a vertical axis. A vertical magnetic field is imposed. The onset of Rayleigh-Bénard convection in this system is a classical problem of magnetohydrodynamics. At present it is a subject of intense investigation because of its importance for astrophysical and geophysical applications. The system in a dimensionless form is characterized by the following parameters: the Rayleigh number, R (measuring the amplitude of thermal buoyancy forces), the Prandtl number, P (the ratio of kinematic viscosity to thermal diffusivity), the magnetic Prandtl number, P_m (the ratio of kinematic viscosity to magnetic diffusivity), the Chandrasekhar number, Q (proportional to the square of the amplitude of the imposed magnetic field), and the square root of the Taylor number $\tau=\mathrm{Ta}^{1/2}$ (proportional to the speed of rotation). Instead of the magnetic Prandtl number we employ the Roberts number $q=P_m/P$. Rigid electrically insulating horizontal boundaries held at constant temperatures are assumed.

For small Rayleigh numbers, i.e., for a small difference of temperatures at the horizontal boundaries, the fluid is at rest and heat is transported by thermal diffusion only. When the Rayleigh number exceeds the critical value, a fluid motion sets in. Without rotation or an imposed magnetic field, the instability is monotonic and the flow takes the form of stable rolls. In a rotating layer or in the presence of an external magnetic field, the onset of convection can be oscillatory. If the onset is steady, the emerging convective rolls can be unstable, and then the flow exhibits other types of behavior.

In this paper we address the question for which parameter values rolls are observed at the onset of convection in a rotating fluid layer with an imposed magnetic field. Only stability of rolls of the critical wave number is examined. Bifurcating rolls are stable near the onset, if the following conditions are satisfied: the mode, becoming unstable the first, is steady; rolls bifurcate supercritically; they are stable to perturbations of the form of rolls rotated by an arbitrary angle. We derive inequalities characterizing each of the three conditions and identify numerically regions in the (P,τ) plane, where they are satisfied, for several fixed values of q and Q.

Without both rotation and an imposed magnetic field, instability of the trivial steady state is monotonic [1]. In a rotating layer, the instability is oscillatory for small values of P and large enough τ. The boundary in the (P,τ) plane between the monotonic and oscillatory onset of convection was computed by Clune and Knobloch [2]. In a layer with an imposed vertical magnetic field, the instability is oscillatory for large Roberts numbers [1]. Weeks and Zhang [3] computed the critical Rayleigh number for various boundary conditions for magnetic field for several sets of other parameter values. Roberts and Zhang [4] explored the limit of small viscosity and magnetic diffusivity.

The combined effect of rotation and an imposed magnetic field on the linear stability was not investigated in such details. Eltayeb [5] studied analytically the asymptotics of the critical Rayleigh number in the limit of large Ta and Q. Critical Rayleigh numbers as a function of τ for $P=0.023$, $P_m=1.5\times10^{-6}$ and four different values of Q were computed by Zhang *et al.* [6]. Their results agreed well with the experiments of Aurnou and Olson [7]: the critical mode is steady for small and moderate τ, and oscillatory for large τ. The competition between steady and oscillatory modes at the onset of rotating magnetoconvection was considered by Podvigina [8]. Boundaries on the (P,τ) plane between the regions of monotonic and oscillatory onset were computed *ibid.* for several pairs of Q and q. In the present paper, we consider different sets of parameter values.

Weakly nonlinear stability was studied in detail only for nonmagnetic rotating convection. In the limit $P\to\infty$, rolls are stable at the onset of convection in a layer with stress-free boundaries for $\mathrm{Ta}<2285$ [9]. Stability of rolls in a layer with rigid boundaries was examined for several finite P by Clever and Busse [10]; they found that a strong reduction of the domain of stable rolls in the (k,R) plane (here k is the wave number of rolls) occurs, as the rotation rate is in-

creased. They also showed that a subcritical finite-amplitude convection is possible for $P<1$. Clune and Knobloch [2] computed a bifurcation diagram in the (P,τ) plane for rotating convection; in particular, they determined the boundary between subcritical and supercritical bifurcations of rolls. According to their diagram, subcritical bifurcations of rolls are also possible for $P>1$. This contradicts the results of [10], which were, however, confirmed by Bajaj *et al.* [11]: according to [11], subcritical bifurcations of rolls are possible only for $P<0.33$.

Stability of flows near the onset of convection in a layer with an imposed vertical magnetic field was first studied by Lortz [12], who derived a necessary condition for stability of small-amplitude solutions. Stability of rolls for boundary conditions on horizontal boundaries, different from those considered in present paper, was investigated by Clune and Knobloch [13], see also a review by Proctor [14].

In this paper we compute bifurcation diagrams for rotating convection [in the (P,τ) plane], magnetoconvection [in the (P,Q) and (q,Q) planes] and rotating magnetoconvection [in the (P,τ) plane]. We find that if rolls bifurcate supercritically and they are unstable, the convective system does not necessarily exhibit the behavior, typical for the Küppers-Lortz instability, that involves domains of small-amplitude rolls incessantly replacing each other. Such behavior is related to existence of heteroclinic cycles connecting the roll states. Other possibilities are: stable patterns that are sums (in the leading order) of two rolls rotated by a finite angle (e.g., squares); unstable patterns (of the same structure) observed during some stages of the temporal evolution, because they are involved into heteroclinic cycles together with rolls; or finite-amplitude regimes emerging near the onset.

To calculate the critical Rayleigh number R_c, we follow the approach that Pellew and Southwell [15] employed for calculation of critical values in a layer without rotation and magnetic field, also employed by Clune and Knobloch [2], Weeks and Zhang [3] and Zhang *et al.* [6]. A mode is a finite sum of products of trigonometric functions and exponential functions with unknown coefficients. Substituting the sum into the boundary conditions and linearized equations defining a critical mode, and solving numerically the resultant system of equations in the coefficients and exponents, we obtain, for a given horizontal wave number of the mode, k, the critical Rayleigh numbers $R^s(k)$ and $R^o(k)$ for the onset of monotonic and oscillatory instabilities. (P, P_m, τ, and Q are supposed to be fixed in these computations.) Calculating the minima of $R^s(k)$ and $R^o(k)$ over k and comparing them, we determine the type of the first instability and the respective critical values, R_c and k_c. {Following a long established tradition—see, for instance [10]—we call indiscriminately all the three values, R_c, $R^s(k)$, and $R^o(k)$, the critical Rayleigh numbers.}

We determine the direction of bifurcation of the rolls branch and its stability from amplitude equations, as was done by Clune and Knobloch [2,13]. The equations are derived by the center manifold reduction. In order to study stability of a roll to the same pattern rotated (relative the roll under examination) by angles $\pm\alpha$, we impose a rhombic periodicity cell in the horizontal directions with the angle α (varying from 0 to $\pi/2$) between the sides of the rhomb.

In experiments, layers infinite in horizontal directions cannot be implemented, and the onset of convection in a rotating layer often occurs in the form of traveling waves attached to vertical sidewalls [16–18]. In a sufficiently large container, nonlinear patterns related to both modes can coexist independently in different parts of the container (bulk modes in the middle and sidewall modes near the vertical boundary) [17,18]. The onset of convection via a traveling sidewall mode in the presence of a vertical magnetic field for a variety of boundary conditions for temperature on the vertical boundary was reported in [19]. We do not consider sidewall modes here.

The paper is organized as follows. In Sec. II the basic equations governing convection and the boundary conditions are reminded. In Sec. III we solve the linear stability problem for the trivial steady state, and in Sec. IV the weakly nonlinear problem. In Secs. III and IV the cases of rotating convection, magnetoconvection, and rotating magnetoconvection are considered in separate subsections. Each subsection is comprised of two parts: a mathematical derivation of equations for the critical parameter values, and numerical results on the regions of stability and patterns of convection emerging at the onset. These two, mathematical and physical, parts can be read separately.

II. STATEMENT OF THE PROBLEM

The fields obey the Navier-Stokes equation

$$\frac{\partial \mathbf{v}}{\partial t} = \mathbf{v}\times(\boldsymbol{\nabla}\times\mathbf{v}) + P\tau\mathbf{v}\times\mathbf{e}_z + P\Delta\mathbf{v} + PR\theta\mathbf{e}_z - \boldsymbol{\nabla}\tilde{p} + PQq^{-1}(\boldsymbol{\nabla}\times\mathbf{B})\times\mathbf{B}, \tag{1}$$

the heat transfer equation

$$\frac{\partial \theta}{\partial t} = -(\mathbf{v}\cdot\boldsymbol{\nabla})\theta + v_z + \Delta\theta \tag{2}$$

and the magnetic induction equation

$$\frac{\partial \mathbf{B}}{\partial t} = \boldsymbol{\nabla}\times(\mathbf{v}\times\mathbf{B}) + q^{-1}\Delta\mathbf{B}. \tag{3}$$

The fluid is incompressible and magnetic field is solenoidal,

$$\boldsymbol{\nabla}\cdot\mathbf{v} = 0, \quad \boldsymbol{\nabla}\cdot\mathbf{B} = 0. \tag{4}$$

Here $\mathbf{v}$ denotes the flow velocity, $\mathbf{B}$ the magnetic field and θ the difference between the flow temperature and the linear temperature profile.

The equations involve the following dimensionless parameters,

$$P = \frac{\nu}{\kappa}, \quad P_m = \frac{\nu}{\mu}, \quad R = \frac{\alpha g d^3}{\nu\kappa}\delta T, \quad \tau = \frac{2\Omega d^2}{\nu}, \quad Q = \frac{\sigma B_0^2 d^2}{\rho\nu}.$$

In the dimensionless form, the units of length and time are d and d^2/κ, respectively; θ is measured in the units of the temperature difference δT between the lower and upper boundaries of the layer, and $\mathbf{B}$ in the units of $\sqrt{\mu_0\rho}\kappa/d$. Here d is the width of the layer, κ is thermal diffusivity, μ_0 is

vacuum magnetic permeability, ρ is mass density, ν is kinematic viscosity, α is volumetric expansion coefficient, g is gravity acceleration, and η is magnetic diffusivity.

Denote $\mathbf{b}=\mathbf{B}-\mathbf{e}_z$, the difference between the magnetic field $\mathbf{B}$ and the imposed field $\mathbf{e}_z$. Equations (1)–(3) can be represented as

$$\frac{\partial \mathbf{w}}{\partial t} = L\mathbf{w} + N(\mathbf{w},\mathbf{w}), \tag{5}$$

where

$$\mathbf{w} = (\mathbf{v}, \theta, \mathbf{b}) \tag{6}$$

is a seven-component vector field,

$$L\mathbf{w} = \begin{pmatrix} P\Delta\mathbf{v} + PR\theta\mathbf{e}_z - \nabla\tilde{p} + PQq^{-1}\dfrac{\partial \mathbf{b}}{\partial z} + P\tau\mathbf{v}\times\mathbf{e}_z \\ v_z + \Delta\theta \\ \dfrac{\partial \mathbf{v}}{\partial z} + q^{-1}\Delta\mathbf{b} \end{pmatrix}, \tag{7}$$

$$N(\mathbf{w}_1,\mathbf{w}_2) = \frac{1}{2}\begin{pmatrix} \mathbf{v}_1\times(\nabla\times\mathbf{v}_2) + \mathbf{v}_2\times(\nabla\times\mathbf{v}_1) + PQq^{-1}[(\nabla\times\mathbf{b}_1)\times\mathbf{b}_2 + (\nabla\times\mathbf{b}_2)\times\mathbf{b}_1] - \nabla p \\ -(\mathbf{v}_1\cdot\nabla)\theta_2 - (\mathbf{v}_2\cdot\nabla)\theta_1 \\ \nabla\times(\mathbf{v}_1\times\mathbf{b}_2) + \nabla\times(\mathbf{v}_2\times\mathbf{b}_1) \end{pmatrix}. \tag{8}$$

The flow satisfies the no-slip conditions on the horizontal boundaries, kept at constant temperatures,

$$v_x = v_y = v_z = 0, \quad \theta = 0 \quad \text{at } z = \pm\frac{1}{2}. \tag{9}$$

The medium outside the layer is perfectly insulating,

$$\mathbf{b}(x,z) = -\nabla\phi(x,z)\left(z = \pm\frac{1}{2}\right),$$
$$\Delta\phi(x,z) = 0\left(|z| > \frac{1}{2}\right), \quad \phi(x,z) \to 0 (|z| \to \infty). \tag{10}$$

In the case of convection without magnetic field, we consider the system [Eq. (5)] restricted onto the space of four-component fields

$$\mathbf{w}^{\mathrm{rc}} = (\mathbf{v}, \theta). \tag{11}$$

The restrictions of the operators L and N are

$$L^{\mathrm{rc}}\mathbf{w}^{\mathrm{rc}} = \begin{pmatrix} P\Delta\mathbf{v} + PR\theta\mathbf{e}_z - \nabla\tilde{p} + P\tau\mathbf{v}\times\mathbf{e}_z \\ v_z + \Delta\theta \end{pmatrix}, \tag{12}$$

$$N^{\mathrm{rc}}(\mathbf{w}_1^{\mathrm{rc}},\mathbf{w}_2^{\mathrm{rc}}) = \frac{1}{2}\begin{pmatrix} \mathbf{v}_1\times(\nabla\times\mathbf{v}_2) + \mathbf{v}_2\times(\nabla\times\mathbf{v}_1) - \nabla p \\ -(\mathbf{v}_1\cdot\nabla)\theta_2 - (\mathbf{v}_2\cdot\nabla)\theta_1 \end{pmatrix}. \tag{13}$$

The system [Eqs. (5)–(10)] [as well as Eqs. (5), (11)–(13), and (9) in the case of rotating convection in the absence of magnetic field] has a trivial steady state $\mathbf{w}=0$ ($\mathbf{w}^{\mathrm{rc}}=0$, respectively), whose stability is determined by the dominant eigenvalues of Eq. (7) [or Eq. (12), respectively]. The steady state becomes unstable when an eigenvalue crosses the imaginary axis. In the next section we determine when this happens.

III. LINEAR STABILITY OF THE TRIVIAL STEADY STATE

We study eigenmodes depending on two variables, x and z. In each linear problem we consider the operator of linearization L [Eq. (7)] [or L^{rc} Eq. (12), if a magnetic field is absent] restricted onto an invariant subspace of vector fields with a prescribed periodicity in the horizontal direction. Because of the structure of these operators, their domains can be decomposed into direct sums of vector fields proportional to $\sin kx$ and $\cos kx$ (where the wave number k is compatible with the imposed periodicity). Furthermore, the operators have constant coefficients; substituting the ansatz

$$\sum_{n\geq 0} (f_n^s \sin nkx + f_n^c \cos nkx) \tag{14}$$

into the eigenvalue equation for Eq. (7) we find that each $f_n^s(z)$ and $f_n^c(z)$ are eigenfunctions of a second order (ordinary) differential operator with constant coefficients. Consequently, generically $f_n^s(z)$ and $f_n^c(z)$ are sums of exponents in z. Note that these arguments are not affected by the requirement to satisfy whichever boundary conditions at the horizontal boundaries.

A. Convection with rotation

1. Derivation of the equation for the stability boundary: The steady onset of convection

The critical mode satisfies the equation

$$L^{\mathrm{rc}}\mathbf{w}^{\mathrm{rc}} = 0 \tag{15}$$

for monotonic instability and

$$L^{\mathrm{rc}}\mathbf{w}^{\mathrm{rc}} = \mathrm{i}\omega\mathbf{w}^{\mathrm{rc}}, \quad \omega \neq 0, \tag{16}$$

for oscillatory instability.

Following the arguments in the preamble of the present section, we employ four-component vector fields

$$\mathbf{f}_1(k,\gamma)=\begin{pmatrix} -\frac{\gamma}{k}e^{\gamma z}\sin kx \\ 0 \\ e^{\gamma z}\cos kx \\ 0 \end{pmatrix},$$

$$\mathbf{f}_2(k,\gamma)=\begin{pmatrix} 0 \\ e^{\gamma z}\sin kx \\ 0 \\ 0 \end{pmatrix}, \quad \mathbf{f}_3(k,\gamma)=\begin{pmatrix} 0 \\ 0 \\ 0 \\ e^{\gamma z}\cos kx \end{pmatrix}. \tag{17}$$

Note that the solenoidality condition for the flow forces us to join the x and z components of the flow into a single vector, $\mathbf{f}_1$. The linearity of the problem and the structure of the operator of linearization imply that it suffices to consider a single term in the sum [Eq. (14)].

For $\gamma \neq \pm k$, the subspace $F(k,\gamma)$ spanned by $\mathbf{f}_j(k,\gamma)$, $j=1,2,3$, is L^{rc}-invariant. The matrix of L^{rc} acting on $F(k,\gamma)$ is

$$\begin{pmatrix} P(\gamma^2-k^2) & -\frac{\tau\gamma k P}{\gamma^2-k^2} & -\frac{PRk^2}{\gamma^2-k^2} \\ -\frac{\tau\gamma P}{k} & P(\gamma^2-k^2) & 0 \\ 1 & 0 & (\gamma^2-k^2) \end{pmatrix}. \tag{18}$$

L^{rc} possesses a nontrivial kernel in $F(k,\gamma)$, if the determinant of Eq. (18) vanishes, i.e.,

$$X^3+\tau^2 X+\tau^2 k^2+Rk^2=0, \tag{19}$$

where $X=\gamma^2-k^2$. If $\gamma=\pm k$, then

$$L^{\mathrm{rc}}[\tau\mathbf{f}_2(k,\gamma)\pm R\mathbf{f}_3(k,\gamma)]=0. \tag{20}$$

Therefore, a solution to Eq. (15) is sought in the form

$$\mathbf{w}^{\mathrm{rc}}=\sum_{j,l=1}^{3,8} A_{jl}\mathbf{f}_j(k,\gamma_l), \tag{21}$$

where

$$\gamma_1=k, \quad \gamma_2=-k, \quad \gamma_{2s+1}=-\gamma_{2s+2}=(X_s+k^2)^{1/2}, \quad s=1,2,3, \tag{22}$$

and X_s are roots of Eq. (19). By virtue of Eqs. (18) and (20), Eq. (21) is a solution to Eq. (15) if the coefficients A_{jl} satisfy

$$A_{11}=A_{12}=0, \quad A_{21}=-\frac{R}{\tau}A_{31}, \quad A_{22}=\frac{R}{\tau}A_{32},$$

$$A_{2l}=-\frac{\tau\gamma_l}{k(\gamma_l^2-k^2)}A_{1l}, \quad A_{3l}=-\frac{1}{(\gamma_l^2-k^2)}A_{1l}, \quad l=3,\ldots,8. \tag{23}$$

We seek an eigenmode [Eq. (21)] satisfying boundary conditions [Eq. (9)]. Substitution of Eq. (21) into Eq. (9) yields a system of linear homogeneous equations in A_{1l}, $l=1,\ldots,8$,

$$\sum_{l=1}^{8} e^{\pm\gamma_l/2}A_{jl}=0, \quad j=1,2,3, \quad \sum_{l=1}^{8}\frac{\gamma_l}{k}e^{\pm\gamma_l/2}A_{1l}=0. \tag{24}$$

Let the eigenmode [Eq. (21)] be even in z (understanding *even* and *odd* in the sense of Chandrasekhar [1]),

$$v_x(z)=-v_x(-z), \quad -v_y(z)=v_y(-z),$$

$$v_z(z)=v_z(-z), \quad \theta(z)=\theta(-z). \tag{25}$$

If Eq. (21) is an even eigenmode and γ_l satisfies Eq. (22), then $A_{21}=-A_{22}$ and $A_{1,2s+1}=A_{1,2s+2}$, $s=1,2,3$. Hence, Eq. (23) implies that Eq. (24) is a system of four homogeneous equations in four unknown quantities: A_{21}, A_{13}, A_{15}, and A_{17}. It has a nonzero solution if

$$\det\begin{pmatrix} 0 & 1 & 1 & 1 \\ 0 & \gamma_3\tanh\gamma_3/2 & \gamma_5\tanh\gamma_5/2 & \gamma_7\tanh\gamma_7/2 \\ \tau & \frac{1}{\gamma_3^2-k^2} & \frac{1}{\gamma_5^2-k^2} & \frac{1}{\gamma_7^2-k^2} \\ -Rk\tanh k/2 & \frac{\tau\gamma_3\tanh\gamma_3/2}{\gamma_3^2-k^2} & \frac{\tau\gamma_5\tanh\gamma_5/2}{\gamma_5^2-k^2} & \frac{\tau\gamma_7\tanh\gamma_7/2}{\gamma_7^2-k^2} \end{pmatrix}=0. \tag{26}$$

For a given k (and a fixed τ), the critical value $R^s(k)$ is a solution to Eq. (26), where γ_l, $l=3,5,7$, are defined by Eqs. (19) and (22). Evaluating the minimum of $R^s(k)$ over k, we determine the critical Rayleigh number R_c^s and the critical wave number k_c^s for monotonic instability.

We have carried out similar calculations for an odd mode, and found that the respective critical Rayleigh number is always larger than for the even mode. This remains true for the oscillatory instability, as well as for convection with an imposed magnetic field. Therefore, only even modes are im-

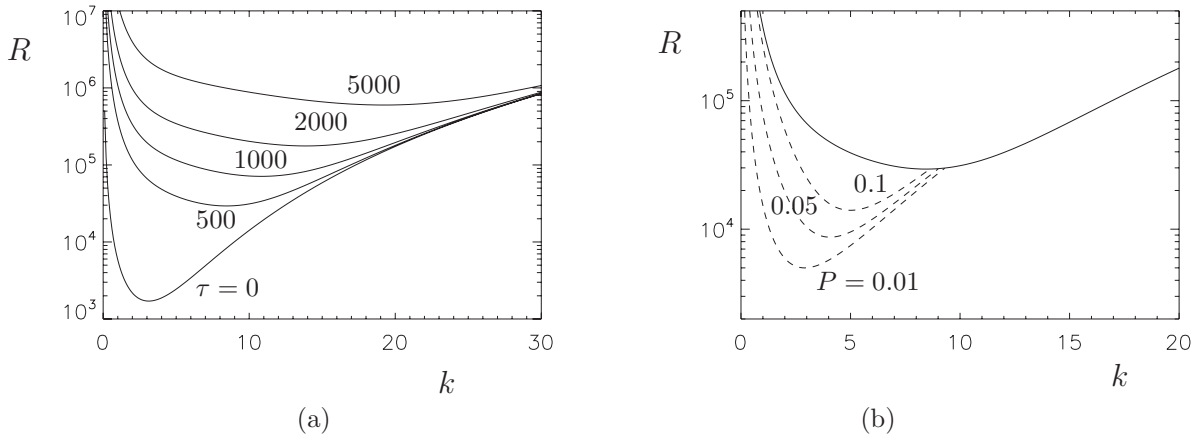

FIG. 1. Critical Rayleigh numbers as functions of k in rotating convection for (a) τ=0, 500, 1000, 2000, 5000; (b) τ=500 and P =0.01, 0.05, 0.1. Solid line: $R^s(k)$ (stationary mode); dashed line: $R^o(k)$ (oscillatory mode).

portant near the onset of convection and only even modes are discussed in this paper.

2. Derivation of the equation for the stability boundary: The oscillatory onset of convection

A critical mode for oscillatory instability is also sought in the form Eq. (21). As in the case of monotonic instability, the eigenvalue equation (16) has a nontrivial solution in $F(k,\gamma)$, where

$$\gamma_{2s-1} = -\gamma_{2s} = (X_s + k^2)^{1/2}, \quad s = 1,2,3,4, \tag{27}$$

and X_s are roots of the equation

$$(PX - i\omega)^2(X - i\omega)X + P^2\tau^2(X - i\omega)(X + k^2) + PRk^2(PX - i\omega) = 0. \tag{28}$$

The coefficients A_{jl} of the eigenmode [Eq. (21)] satisfy the relations

$$A_{2l} = -\frac{P\tau\gamma_l}{k(P(\gamma_l^2 - k^2) - i\omega)}A_{1l},$$

$$A_{3l} = -\frac{1}{(\gamma_l^2 - k^2) - i\omega}A_{1l}, \quad l = 1, \ldots, 8. \tag{29}$$

Together, relations (27)–(29) are equivalent to the eigenvalue Eq. (16) for the critical mode [Eq. (21)] restricted to the subspace $F(k,\gamma)$. The mode satisfies the boundary conditions [Eq. (9)] if

$$\det \mathcal{A} = 0, \tag{30}$$

where the entries of the matrix $\mathcal{A}$ are

$$\mathcal{A}_{1,s} = 1, \quad \mathcal{A}_{2,s} = \gamma_{2s-1}\tanh\gamma_{2s-1}/2,$$

$$\mathcal{A}_{3,s} = \frac{1}{i\omega - (\gamma_{2s-1}^2 - k^2)}, \quad \mathcal{A}_{4,s} = \frac{\gamma_{2s-1}\tanh\gamma_{2s-1}/2}{i\omega - P(\gamma_{2s-1}^2 - k^2)}, \quad s = 1,2,3,4. \tag{31}$$

The determinant of $\mathcal{A}$ is a complex-valued function of two real variables, R and ω (note that γ_l and X_s are complex). Consequently, Eq. (30) determines $R^o(k)$ and $\omega^o(k)$. Minimizing $R^o(k)$ over k we find R_c^o and k_c^o. Comparison with R_c^s yields the critical Rayleigh number R_c and the critical wave number k_c for the onset of convection.

For an individual k, we solved Eq. (26) in $R^s(k)$ by bisection; convergence was so fast, that no more efficient methods were required. Broyden's method (see [20]) was used to solve Eq. (30) in two variables, $R^o(k)$ and $\omega^o(k)$; convergence was fast for good initial approximations, usually acquired by continuation in parameters. These methods were also employed to make computations for the problems of magnetoconvection in the absence and presence of rotation, which are discussed in subsequent subsections. In total, the computations presented in this paper consumed about two weeks of CPU time of a single Pentium III processor.

3. Numerical results

The critical values $R^s(k)$ are shown for several values of τ and a range of k in Fig. 1(a); $R^s(k)$, R_c^s, and the critical wave number increase with τ. The critical values $R^o(k)$, R_c^o and k_c^o decrease with P [see Fig. 1(b); $R^s(k)$ is independent of the Prandtl number]. Oscillatory branches terminate on the steady-state branch; the frequency of oscillations vanishes at the junction.

B. Convection with magnetic field, no rotation

We denote by L^{mc} the operator L for τ=0. The domain of L^{mc} splits into a direct sum of invariant subspaces spanned by vector fields $(\mathbf{v},0,\mathbf{b})$, where $\mathbf{v}$ and $\mathbf{b}$ are toroidal, and by $(\mathbf{v},\theta,\mathbf{b})$, where $\mathbf{v}$ and $\mathbf{b}$ are poloidal. Eigenvalues of L^{mc} associated with eigenvectors from the former subspace are always strictly negative [14]. We consider, therefore, only eigenvectors from the latter subspace. The critical modes for monotonic and oscillatory instabilities satisfy

$$L^{\mathrm{mc}}\mathbf{w}^{\mathrm{mc}} = 0 \tag{32}$$

and

$$L^{\mathrm{mc}}\mathbf{w}^{\mathrm{mc}} = i\omega\mathbf{w}^{\mathrm{mc}}, \quad \omega \neq 0, \tag{33}$$

respectively.

1. Derivation of the equation for the stability boundary: The steady onset of magnetoconvection

Let k be the horizontal wave number of a critical mode. In this subsection we denote by $\mathbf{f}_j(k,\gamma)$, where $j=1,3$, 7-component vector fields defined by Eq. (17) and having zero magnetic components. We also define a vector field $\mathbf{f}_4(k,\gamma)$ by the relations

$$\mathbf{f}_4^{(1-4)}(k,\gamma)=0, \quad \mathbf{f}_4^{(5-7)}(k,\gamma)=\begin{pmatrix} -\frac{\gamma}{k}e^{\gamma z}\sin kx \\ 0 \\ e^{\gamma z}\cos kx \end{pmatrix}. \quad (34)$$

Here $\mathbf{f}^{(m-n)}$ denotes an $(n-m+1)$-component vector $(f^m,f^{m+1},\ldots,f^n)$, comprised of the components of $\mathbf{f}$. Consequently, $\mathbf{f}_4^{(1-4)}$ is the flow and temperature part and $\mathbf{f}_4^{(5-7)}$ the magnetic part of the field $\mathbf{f}_4$.

The subspace $F(k,\gamma)$ spanned by $\mathbf{f}_j(k,\gamma)$, $j=1,3,4$, for $\gamma\neq\pm k$ is L^{mc}-invariant. The matrix of L^{mc} in this subspace is

$$\begin{pmatrix} P(\gamma^2-k^2) & -\frac{PRk^2}{\gamma^2-k^2} & PQq^{-1}\gamma \\ 1 & (\gamma^2-k^2) & 0 \\ \gamma & 0 & q^{-1}(\gamma^2-k^2) \end{pmatrix}. \quad (35)$$

The operator L^{mc} possesses a nontrivial kernel, if the determinant of Eq. (35) vanishes, i.e.,

$$X^3-QX(X+k^2)+Rk^2=0, \quad (36)$$

where $X=\gamma^2-k^2$. For $\gamma=\pm k$,

$$L^{\mathrm{mc}}\mathbf{f}_4(k,\pm k)=0. \quad (37)$$

Consider a critical mode of the form

$$\mathbf{w}=\sum_{j=1,3,4}\sum_{l=1}^{8}A_{jl}\mathbf{f}_j(k,\gamma_l), \quad (38)$$

where

$$\gamma_{2s-1}=-\gamma_{2s}=(X_s+k^2)^{1/2}, \quad s=1,2,3, \quad \gamma_7=k, \quad \gamma_8=-k, \quad (39)$$

and X_s are roots of Eq. (36). Coefficients of the critical mode [Eq. (38)] satisfy

$$A_{3l}=-\frac{1}{\gamma_l^2-k^2}A_{1l}, \quad A_{4l}=-\frac{\gamma_l q}{\gamma_l^2-k^2}A_{1l}, \quad l=1,\ldots,6,$$

$$A_{1l}=A_{3l}=0, \quad l=7,8. \quad (40)$$

Relations (36), (39), and (40) together are equivalent to the eigenvalue equation (32) for the critical mode [Eq. (38)] restricted to the subspace $F(k,\gamma)$.

An even critical mode [Eq. (38)] satisfies the boundary conditions [Eq. (9)], if the system

$$\sum_{l=1}^{6}e^{\gamma_l/2}A_{jl}=0, \quad j=1,3, \quad \sum_{l=1}^{6}\frac{\gamma_l}{k}e^{\gamma_l/2}A_{1l}=0 \quad (41)$$

has a nontrivial solution, i.e.,

$$\det\begin{pmatrix} 1 & 1 & 1 \\ \gamma_1\tanh\gamma_1/2 & \gamma_3\tanh\gamma_3/2 & \gamma_5\tanh\gamma_5/2 \\ \frac{1}{\gamma_1^2-k^2} & \frac{1}{\gamma_3^2-k^2} & \frac{1}{\gamma_5^2-k^2} \end{pmatrix}=0. \quad (42)$$

This equation determines $R^s(k)$.

The boundary condition for magnetic field [Eq. (10)] has not yet been considered. It can be satisfied by adding $\mathbf{f}_4(k,\pm k)$ with an appropriate coefficient [note Eq. (37)]. In view of the structure of the operator L^{mc} [Eq. (7)], the symmetry relations [Eq. (25)] for the flow velocity and temperature in an even mode are compatible with the following symmetry of the magnetic component of an even mode [Eq. (6)]:

$$b_x(z)=b_x(-z), \quad b_y(z)=b_y(-z), \quad b_z(z)=-b_z(-z). \quad (43)$$

For an even or an odd mode it suffices to satisfy the condition on one boundary. The potential of magnetic field [Eq. (10)] in the dielectric half-spaces $\pm z>1/2$ is $\phi=Ce^{\mp kz}\cos kx$, and hence

$$A_{47}=-\frac{1}{2e^{k/2}}\sum_{l=1}^{6}A_{4l}\left(1+\frac{\gamma_l}{k}\right)e^{\gamma_l/2}, \quad A_{48}=-A_{47}. \quad (44)$$

2. Derivation of the equation for the stability boundary: The oscillatory onset of magnetoconvection

We proceed as in the case of rotating convection, considering the eigenvalue equation (33) for an oscillatory mode restricted to the invariant subspace $F(k,\gamma)$ of L^{mc} spanned by vector fields $\mathbf{f}_j(k,\gamma)$. We start by expressing [Eq. (33)] in the terms of relations of coefficients in the expansion of the mode in this basis (not presented here). Considering afterwards the boundary conditions, we find that $R^o(k)$ and $\omega^o(k)$ for oscillatory instability can be determined from the condition $\det\mathcal{A}=0$, where the matrix $\mathcal{A}$ has the following entries:

$$\mathcal{A}_{1s}=1, \quad \mathcal{A}_{2s}=\gamma_{2s-1}\tanh\gamma_{2s-1}/2,$$

$$\mathcal{A}_{3s}=\frac{1}{i\omega-(\gamma_{2s-1}^2-k^2)},$$

$$\mathcal{A}_{4s}=\frac{\gamma_{2s-1}(k\tanh\gamma_{2s-1}/2+\gamma_{2s-1})}{i\omega q-(\gamma_{2s-1}^2-k^2)}, \quad (45)$$

where $\gamma_{2s+1}=-\gamma_{2s+2}=(X_s+k^2)^{1/2}$, and X_s are roots of the equation

$$(PX-i\omega)(X-i\omega q)(X-i\omega)X-PQ(X-i\omega)(X+k^2)X+PRk^2(X-i\omega q)=0. \quad (46)$$

Weeks and Zhang [3] considered linear stability of the trivial steady state in magnetoconvection for various bound-

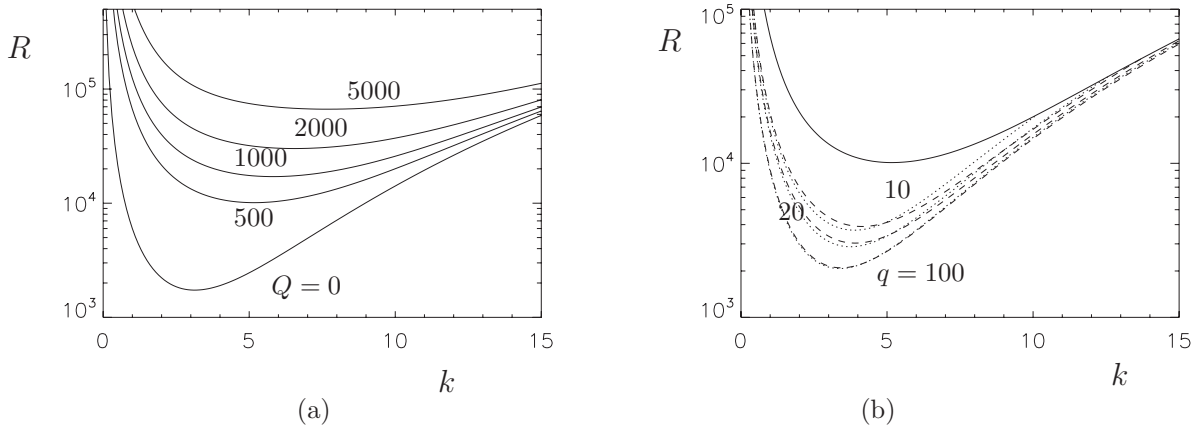

FIG. 2. Critical Rayleigh numbers as functions of k in nonrotating magnetoconvection for (a) $Q=0$, 500, 1000, 2000, 5000; (b) $Q=500$ and $q=10$, 20, 100. Solid line: $R^s(k)$ (stationary mode); dashed ($P=0.5$) and dotted ($P=50$) lines: $R^o(k)$ (oscillatory mode).

ary conditions for magnetic field. They decomposed velocity and magnetic field into poloidal and toroidal parts. Their equations determining the critical values for perfectly insulating boundary conditions are equivalent to our Eqs. (30), (36), (42), (45), and (46), and we have checked our code against several critical Rayleigh numbers and frequencies presented *ibid*. For horizontal boundaries of finite electrical conductivity, the authors *ibid.* expanded an eigenmode of Eq. (48) in an infinite sum of Chebyshev functions in z and employed a finite number of terms in computations. This is unnecessary, since for these conditions the neutral oscillatory mode can be sought as a finite sum [Eq. (38)], and our analysis remains applicable [with $\mathcal{A}_{4s}$ in Eq. (45) replaced by an appropriate expression].

3. Numerical results

The critical values $R^s(k)$ for several values of Q and a range of k are shown in Fig. 2(a); $R^s(k)$, R_c^s and the critical wave numbers increase with Q. The values $R^o(k)$ for oscillatory instability depend on P, q, and Q [see Fig. 2(b)]; $R^o(k)$, R_c and the critical wave number decrease as q increases. Oscillatory instability is possible only for $q>1$. Dependence on P is visually undetectable for large q; for moderate q, R_c slightly decreases as P increases.

C. Rotating convection with magnetic field

The critical modes for monotonic and oscillatory instabilities satisfy the equations

$$L\mathbf{w} = 0 \tag{47}$$

and

$$L\mathbf{w} = \mathrm{i}\omega\mathbf{w}, \quad \omega \neq 0, \tag{48}$$

respectively, with the operator of linearization L [Eq. (7)] acting in the space of seven-component vector fields [Eq. (6)].

1. Equation for the stability boundary: The steady onset of magnetoconvection in the presence of rotation

The subspace spanned by $\mathbf{f}_j$, $j=1,\ldots,4$ [see Eqs. (17) and (34)] and

$$\mathbf{f}_5^{1-4}(k,\gamma) = 0, \quad \mathbf{f}_5^{5-7}(k,\gamma) = \begin{pmatrix} 0 \\ e^{\gamma z}\sin kx \\ 0 \end{pmatrix}$$

is L invariant. The matrix of the operator L restricted to this subspace is

$$\begin{pmatrix} P(\gamma^2-k^2) & -\dfrac{\tau P\gamma k}{\gamma^2-k^2} & -\dfrac{RPk^2}{\gamma^2-k^2} & PQq^{-1}\gamma & 0 \\ -\dfrac{\tau P\gamma}{k} & P(\gamma^2-k^2) & 0 & 0 & PQq^{-1}\gamma \\ 1 & 0 & (\gamma^2-k^2) & 0 & 0 \\ \gamma & 0 & 0 & q^{-1}(\gamma^2-k^2) & 0 \\ 0 & \gamma & 0 & 0 & q^{-1}(\gamma^2-k^2) \end{pmatrix}. \tag{49}$$

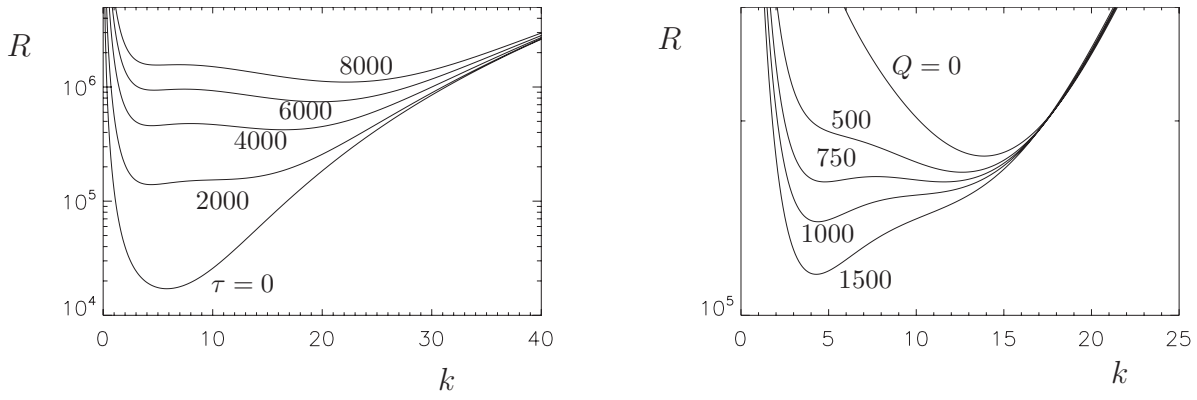

FIG. 3. Critical Rayleigh number $R^s(k)$ (stationary mode) as a function of k in rotating magnetoconvection for (a) $Q=1000$ and $\tau=0$, 2000, 4000, 6000, 8000; (b) $\tau=2000$ and $Q=0$, 500, 750, 1000, 1500.

We consider critical modes for monotonic and oscillatory instabilities of the form

$$\mathbf{w} = \sum_{j,l=1}^{5,10} A_{jl}\mathbf{f}_j(k,\gamma_l). \tag{50}$$

Proceeding as in Secs. III A and III B, we find that for monotonic instability $R^s(k)$ is a solution to the equation $\det \mathcal{A}=0$, where the matrix $\mathcal{A}$ has the entries

$$\mathcal{A}_{1s}=1, \quad \mathcal{A}_{2s}=\gamma_{2s-1}\tanh\gamma_{2s-1}/2, \quad \mathcal{A}_{3s}=\frac{1}{\gamma_{2s-1}^2-k^2},$$

$$\mathcal{A}_{4s}=\frac{\gamma_{2s-1}\tanh\gamma_{2s-1}/2}{\gamma_{2s-1}^2-k^2}, \quad \mathcal{A}_{5s}=\frac{\gamma_{2s-1}^2}{(\gamma_{2s-1}^2-k^2)^2-Q\gamma_{2s-1}^2}, \quad s=1-5, \tag{51}$$

$\gamma_{2s-1}=-\gamma_{2s}=(X_s+k^2)^{1/2}$, and X_s are roots of the equation

$$[X^3-QX(X+k^2)+Rk^2][X^2-Q(X+k^2)]+\tau^2X^2(X+k^2)=0. \tag{52}$$

2. Equation for the stability boundary: The oscillatory onset of magnetoconvection

For oscillatory instability, $R^o(k)$ and $\omega^o(k)$ satisfy the equation $\det \mathcal{A}=0$, where the matrix $\mathcal{A}$ has the entries

$$\mathcal{A}_{1s}=1, \quad \mathcal{A}_{2s}=\gamma_{2s-1}\tanh\gamma_{2s-1}/2,$$

$$\mathcal{A}_{3s}=\frac{1}{(\gamma_{2s-1}^2-k^2)-i\omega}, \quad \mathcal{A}_{4s}=\frac{\gamma_{2s-1}\tanh\gamma_{2s-1}/2}{P(\gamma_{2s-1}^2-k^2)-i\omega},$$

$$\mathcal{A}_{5s}=\frac{\gamma_{2s-1}(k\tanh\gamma_{2s-1}/2+\gamma_{2s-1})}{i\omega q-(\gamma_{2s-1}^2-k^2)},$$

$$\mathcal{A}_{6s}=\frac{\gamma_{2s-1}^2}{(P(\gamma_{2s-1}^2-k^2)-i\omega)((\gamma_{2s-1}^2-k^2)-i\omega q)-PQ\gamma_{2s-1}^2}, \quad s=1-6, \tag{53}$$

$\gamma_{2s-1}=-\gamma_{2s}=(X_s+k^2)^{1/2}$ and X_s are roots of the equation

$$[(PX-i\omega)(X-i\omega q)(X-i\omega)X-PQ(X-i\omega)(X+k^2)X+PRk^2(X-i\omega q)][(PX-i\omega)(X-i\omega q)-PQ(X+k^2))+P^2\tau^2(X+k^2)(X-i\omega)(X-i\omega q)^2=0. \tag{54}$$

3. Numerical results

Dependence of $R^s(k)$ on τ and Q is shown in Fig. 3. For a fixed Q, $R^s(k)$ increases with τ. For Q and τ large enough, the curve $R^s(k)$ has two local minima; on increasing τ, the global (over k) minimum jumps from the local minimum at a lower k to the minimum at a larger k. For a fixed sufficiently large τ, initially R_c decreases on increasing Q [see Fig. 3(b)]; when Q is large enough (not shown in the figure), R_c grows together with Q. Chandrasekhar [1] found a similar dependence of $R^s(k)$ on k, τ, and Q for rotating magnetoconvection with stress-free horizontal boundaries.

For oscillatory instability, $R^o(k)$ and $\omega^o(k)$ depend not only on τ and Q, but also on P and q. For some parameter values there exist two branches of oscillatory modes (see Fig. 4). Modes constituting the branch for larger k are obtained by continuation in τ from the oscillatory mode of magnetoconvection without rotation (modified Alfvén waves). Modes from the other branch are obtained by continuation in Q from the oscillatory mode of nonmagnetic convection with rotation (thermal inertial waves). We call modes from these two branches *magnetic* and *rotational* oscillatory modes, respectively. The magnetic oscillatory modes exist for sufficiently large q; $R^o(k)$ decreases as q increases, as in nonrotating magnetoconvection. The rotational oscillatory modes exist for small P. $R^o(k)$ grows with P, as in nonmagnetic convection with rotation.

Another interesting feature of oscillatory modes is nonuniqueness of the critical value $R^o(k)$ within a single branch (parametrized by k) for some parameter values, i.e., for some

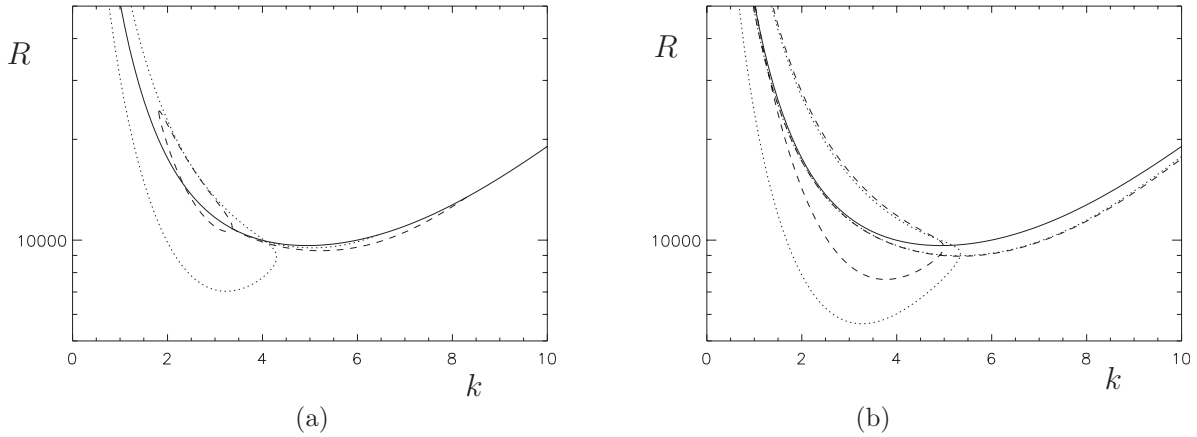

FIG. 4. Critical Rayleigh numbers as functions of k in rotating magnetoconvection for $\tau=200$, $Q=200$ and (a) $q=50$, (b) $q=500$. Solid line: $R^s(k)$ (stationary mode); dashed ($P=0.1$) and dotted ($P=0.05$) lines: $R^o(k)$ (oscillatory mode).

k the trivial state is unstable to oscillatory modes only at a finite interval of Rayleigh numbers. If either rotation, or imposed magnetic field are absent, for a given k and a varying R (other parameters being fixed) there exists at most one neutral oscillatory mode, and then $R^o(k)<R^s(k)$. Typically, for a varying R and other parameters fixed, neutral oscillatory modes exist at a finite interval of k. At the extreme values of k the branch $R^o(k)$ terminates on the $R^s(k)$ branch and at the junction $\omega^o(k)=0$ (unless the left boundary of the interval of existence at $k=0$ is considered). If both rotation and magnetic field are present, then the curve $R^o(k)$ on the (R,k) plane can also turn back at an extreme k; neutral oscillatory modes reside to the left of the turning point, such as plots of critical Rayleigh numbers for rotational oscillatory modes shown in Fig. 4.

Figure 5 illustrates the dependence of $R^o(k)$ on Q. For $Q=10$, the nonuniqueness of $R^o(k)$ is visible in the Figure only for $P=0.15$. For $Q=20$, the nonuniqueness is also seen for $P=0.1$, and for $P=0.15$, the two ends of the $R^o(k)$ branch are linked and produce a closed curve.

The regions on the (P,τ) plane where the first instability is monotonic or oscillatory are shown in Fig. 6 for several values of Q and q. For comparison, the similar region for rotating nonmagnetic convection is shown. Without magnetic field, the onset of convection is oscillatory for small P ($P<0.677$ according to Clune and Knobloch [2]) and sufficiently large τ. With an imposed magnetic field, for small P and sufficiently large τ the onset of convection is also oscillatory. On increasing Q, the boundary of this region of oscillatory instability moves toward larger τ. In this region of parameters, the modes are rotational oscillatory modes.

In another region of oscillatory instability [see Fig. 6(b) for $q=50$], for large P and small τ the modes are magnetic. The region grows on increasing q or Q. For sufficiently large Q and q the two oscillatory regions intersect with formation of two disconnected regions of monotonic onset of convection.

The boundary $\tau^b(P)$ between the monotonic and oscillatory onset of convection on the (P,τ) plane (for fixed Q and q) was computed for rotation modes by the following steps: tabulation of $R_c^s(\tau)=\min_k R^s(k,\tau)$ on a nonuniform grid τ_n; for a given P, determination of τ_n, such that

$$R_c^o(P,\tau_n)\geq R_c^s(\tau_n) \quad \text{and} \quad R_c^s(\tau_{n+1})\geq R_c^o(P,\tau_{n+1}), \quad (55)$$

evaluation of $\tau^b(P)$ by interpolation of $R_c^o(P,\tau)-R_c^s(\tau)$. The same algorithm was applied for magnetic modes, except for both signs $\geq$ in Eq. (55) were replaced by $\leq$.

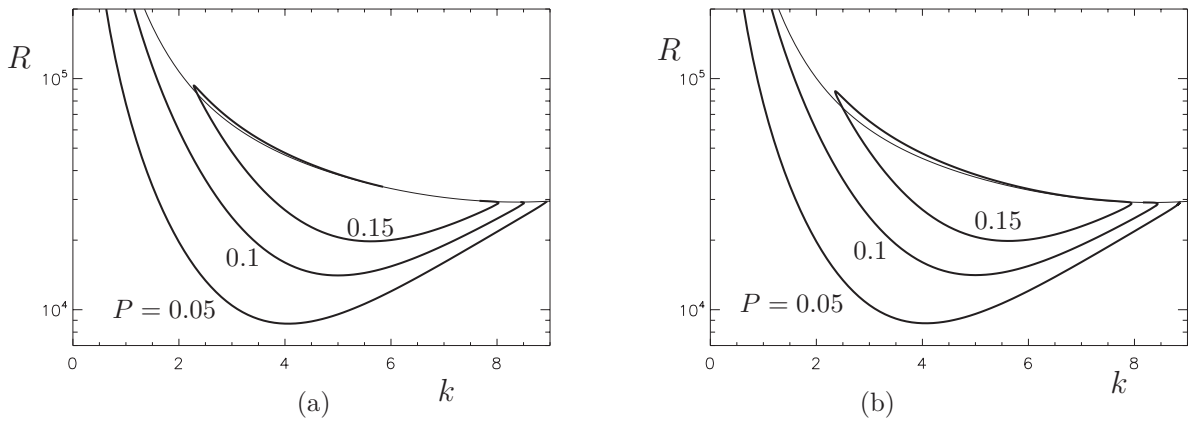

FIG. 5. Critical Rayleigh numbers as functions of k in rotating magnetoconvection for $\tau=200$, $Q=200$ and (a) $q=10$, (b) $q=20$. Thin line: $R^s(k)$ (stationary mode); bold line: $R^o(k)$ (oscillatory mode) for $P=0.15$, 0.1, and 0.05.

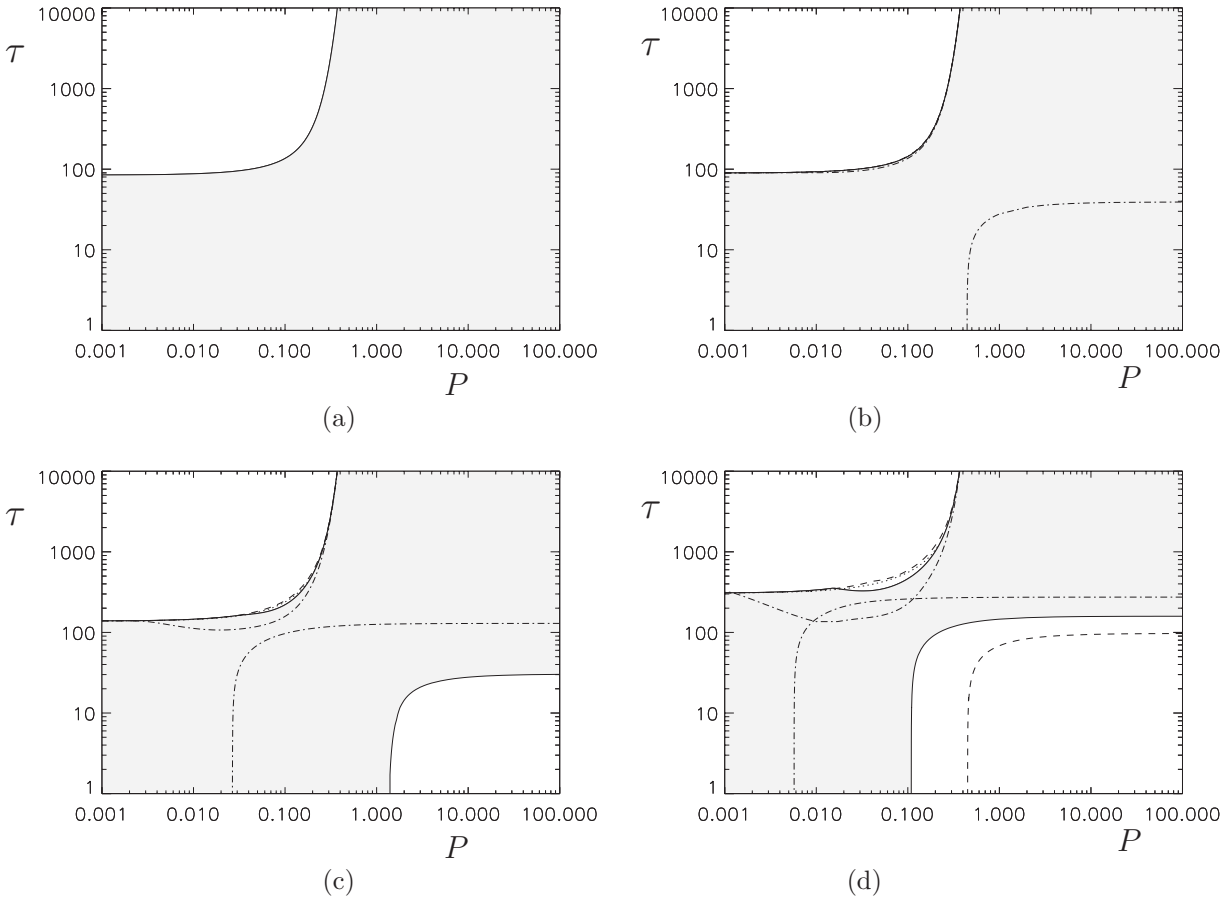

FIG. 6. Boundaries on the (P,τ) plane between the steady and oscillatory onset of (a) rotating nonmagnetic convection and rotating magnetoconvection for (b) $Q=5$, (c) $Q=50$, and (d) $Q=500$. Dotted line: $q=0.01$, dashed line: $q=3$, solid line: $q=5$, dash-dotted line: $q=50$. The region where the onset of convection is steady for $q=5$ is shaded.

IV. WEAKLY NONLINEAR STABILITY

A. Amplitude equations

To study stability of rolls to a similar pattern rotated by angle α, following Clune and Knobloch [2] we consider vector fields, periodic on a rhombic lattice, where the acute angle of the rhomb α varies from 0 to $\pi/2$. The lattice is defined by two horizontal vectors, $(x,y)=\ell(0,1)$ and $(x,y)=\ell(\sin\alpha,-\cos\alpha)$. For $\ell=2\pi/(k_c\sin\alpha)$, rolls with horizontal wave vectors $k_c(1,0)$ and $k_c(\cos\alpha,\sin\alpha)$ are compatible with the lattice. The center eigenspace is spanned by monotonic neutral modes of L (or L^{rc}, or L^{mc}), rolls, calculated in Sec. III C 1 (Sec. III A 1 or Sec. III B 1, respectively). For a slightly supercritical Rayleigh number, truncating at the third order the equations governing the dynamics of the system restricted to the center manifold, we obtain

$$\dot{z}_1=(\lambda+a|z_1|^2+b_1|z_2|^2)z_1,$$

$$\dot{z}_2=(\lambda+a|z_2|^2+b_2|z_1|^2)z_2. \tag{56}$$

The symmetries of the system are translations in the two horizontal directions and inversion $\mathbf{z}\to-\mathbf{z}$. The mapping $z_1\to z_2$ is not a symmetry of the system, but it is a symmetry of the layer without the imposed periodicity and as a result two pairs of equal coefficients emerge in Eq. (56).

The roll solution $(x,0)$ emerging in a bifurcation at $\lambda=0$ satisfies

$$\lambda+ax^2=0.$$

For $a<0$ the bifurcation is supercritical, the branch of the roll solutions exists for $\lambda>0$; they are stable to perturbations of the form $(y,0)$. For $a>0$ the bifurcation is subcritical and the emerging solutions are unstable to such perturbations.

Eigenvalues of the linearization of [Eq. (56)] near the steady state $(x,0)$ are

$$-2\lambda,\quad 0,\quad x^2(b_2-a)\ \text{(twice)}.$$

The double eigenvalue is associated with eigenvectors $(0,z_2)$. Therefore, the rolls $(x,0)$ bifurcating subcritically are stable, if

$$b_2-a<0. \tag{57}$$

The rolls are stable to rolls rotated by the angle $-\alpha$, if

$$b_1-a<0. \tag{58}$$

To examine stability of rolls, we checked numerically the two inequalities for all $0<\alpha\leq\pi/2$. Together, the two conditions imply stability of rolls to any perturbation of the form of a roll.

B. Different types of instabilities

We prove in the Appendix that if rolls bifurcate supercritically then generically the system [Eq. (56)] restricted to $\mathbf{R}^2$ exhibits four different types of behavior. Hence, we distinguish four respective types of instabilities of rolls which can lead to different types of behavior that can be observed in the fluid layer, if rolls bifurcate supercritically (below, numbers i–iv refer to the four types considered in the Appendix):

(I) For $0<\alpha\leq\pi/2$, the case *i* takes place, i.e.,

$$\max_{\alpha} \max[b_1(\alpha)-a, b_2(\alpha)-a] < 0, \tag{59}$$

and rolls are stable at the onset of convection.

(II) For $0<\alpha\leq\pi/2$, the cases i or ii take place, i.e.,

$$\max_{\alpha} \max[b_1(\alpha)-a, b_2(\alpha)-a] > 0,$$

$$\max_{\alpha} \min[b_1(\alpha)-a, b_2(\alpha)-a] < 0. \tag{60}$$

"Domain chaos" typical for Küppers-Lortz instability is observed in experiments. The pattern consists of patches of rolls incessantly replacing each other. Such behavior is attributed to the heteroclinic connections in the dynamical system [Eq. (56)] [21].

(III) For $0<\alpha\leq\pi/2$, cases i, ii, or iii occur, i.e.,

$$\max_{\alpha} \min[b_1(\alpha)-a, b_2(\alpha)-a] > 0,$$

$$\max_{\alpha} \min[b_1(\alpha)b_2(\alpha)-a^2, b_1(\alpha)-a, b_2(\alpha)-a] < 0. \tag{61}$$

Recall that $S_3(\alpha)$ is only *potentially stable*, since [Eq. (A7)] guarantees stability of $S_3(\alpha)$ only with respect to perturbations belonging to the central manifold, namely, to linear combinations of rolls with horizontal wave vectors $k_c(1,0)$ and $k_c(\cos\alpha, \sin\alpha)$. Stability of S_3 to *all* perturbations is an open problem which we do not consider here. Consequently, depending on whether for some α there exist stable steady states $S_3(\alpha)$, two types of behavior can be distinguished:

(IIIa) $S_3(\alpha)$ is stable; therefore, it can be observed in experiments.

(IIIb) $S_3(\alpha)$ is unstable. The behavior observed in experiments can be more complex than the "domain chaos," with intermittant patches of rolls and "rhombic" patterns involved.

(IV) For some α, iv takes place, i.e.,

$$\max_{\alpha} \min[b_1(\alpha)b_2(\alpha)-a^2, b_1(\alpha)-a, b_2(\alpha)-a] > 0. \tag{62}$$

This condition implies that there exist a small perturbation of rolls, whose amplitude increases indefinitely. Consequently, the flows can escape from the neighborhood of the trivial steady state where the CM reduction is valid, and at the onset finite-amplitude flows will be observed.

We stress that the above results only suggest possible types of behavior. They are insufficient for a reliable prediction of what is observed in experiments. This is due to the limitations of the problem that we consider: Our study is restricted to R asymptotically close to R_c and $k=k_c$, however, the values of $R-R_c$ are finite in experiments and thus instability modes of the trivial steady state with $k\neq k_c$ exist; they can give rise to emergence of convective regimes (still rolls) with different stability properties. Multiple attractors are typical for convective systems [21], hence the behavior at large times can depend on the initial conditions. Even if the initial conditions are carefully set as rolls, the instability will follow the mode with the largest growth rate; this dominant mode is a roll rotated by an angle, which does not necessarily coincide with the angle between the two constituent rolls in $S_3(\alpha)$ in area (III). A new investigation is desirable to determine the angle, by which the instability mode associated with the dominant growth rate is rotated. When these two angles are different, this instability can, in principle, prevent the formation of $S_3(\alpha)$. In areas III and IV the Küppers-Lortz instability is possible and its growth rate can be larger than the one of the instability mode resulting in formation of the S_3 patterns in area III, and in the escape of the convective regime from a neighborhood of the rolls in area IV. Finally, we consider an idealized system—an infinite layer—thus excluding the possibility that instabilities near sidewalls are significant. In the three subsections that follow we compute the coefficients a, b_1 and b_2 for different dimensionless parameters of the convective system.

C. Convection with rotation

1. Calculation of coefficients in Eq. (56)

Consider the operator L^{rc} [Eq. (12)] acting in the space $\mathcal{H}^{\mathrm{rc}}_{\alpha}$ of four-component vector fields [Eq. (11)] periodic on a rhombic lattice (see Sec. IV A) and satisfying the boundary conditions [Eq. (9)]. At the steady-state bifurcation of $\mathbf{w}^{\mathrm{rc}} \equiv (\mathbf{v},\theta)=\mathbf{0}$, considered in Sec. III A 1, the operator possesses a four-dimensional kernel called center eigenspace and denoted by X_c. Consider the basis $\{\mathbf{X}_1,\mathbf{X}_2,\mathbf{Y}_1,\mathbf{Y}_2\}$ in X_c, where $\mathbf{X}_1$ is the center eigenvector found in Sec. III A 1. [It is defined by relations (17), (21), and (23) with exponents γ_l satisfying Eqs. (19), (22), and (24).] $\mathbf{X}_2$ is $\mathbf{X}_1$ rotated by the angle α about a vertical axis; $\mathbf{Y}_j$ are $\mathbf{X}_j$ shifted by π/k_c along the directions $\mathbf{e}_x$ and $\cos\alpha\mathbf{e}_x+\sin\alpha\mathbf{e}_y$ for $j=1$ and $j=2$, respectively. (x_1,x_2,y_1,y_2) denote coordinates in this basis.

The center manifold is an invariant manifold tangent to X_c. Near a point of bifurcation the local behavior in the vicinity of $\mathbf{w}^{\mathrm{rc}}=0$ is determined by the dynamics on the center manifold. Locally the center manifold can be represented as a graph of the mapping $\psi: X_c \to X_h$, where X_h is the L^{rc}-invariant complement to X_c in $\mathcal{H}^{\mathrm{rc}}_{\alpha}$. The second-order Taylor expansion is

$$\psi(\mathbf{x},\mathbf{y}) = \sum_{i,j=1}^{2} \xi^1_{ij} x_i x_j + \sum_{i,j=1}^{2} \xi^2_{ij} x_i y_j + \sum_{i,j=1}^{2} \xi^3_{ij} y_i y_j, \tag{63}$$

where $\xi \in X_h$.

Denote by $L^{\mathrm{rc},*}$ the operator adjoint to L^{rc} for the scalar product

$$\mathbf{w}_1 \cdot \mathbf{w}_2 = \mathbf{v}_1 \cdot \mathbf{v}_2 + PR\theta_1 \cdot \theta_2. \tag{64}$$

$L^{\mathrm{rc},*}$ coincides with L^{rc} derived for convection with rotation in the inverse direction. The dual basis $\{\mathbf{X}_1^*, \mathbf{X}_2^*, \mathbf{Y}_1^*, \mathbf{Y}_2^*\}$, can be obtained by changing $\tau \to -\tau$ in Eqs. (23) and (24).

The center manifold coefficients ξ_{1j}^1 satisfy the equations

$$L^{\mathrm{rc}}\xi_{11}^1 + N^{\mathrm{rc}}(\mathbf{X}_1, \mathbf{X}_1) = 0, \quad L^{\mathrm{rc}}\xi_{12}^1 + 2N^{\mathrm{rc}}(\mathbf{X}_1, \mathbf{X}_2) = 0 \tag{65}$$

(they are obtained setting $\omega=0$ in the equations derived in Sec. 2.2 of Podvigina [22]); the remaining ξ_{ij}^s can be found applying the symmetries of the system. A solution to the second Eq. (65) can be found as a sum

$$\xi_{12}^1 = \eta_1 + \eta_2, \tag{66}$$

where

$$L^{\mathrm{rc}}\eta_1 + N^{\mathrm{rc}}(\mathbf{X}_1, \mathbf{X}_2) = 0, \tag{67}$$

η_1 does not necessarily satisfy the boundary conditions [Eq. (9)], and this is compensated for by η_2 satisfying

$$L^{\mathrm{rc}}\eta_2 = 0. \tag{68}$$

Solutions to these problems and all quantities that are of interest for us can be derived as finite sums involving the exponents γ_l and coefficients A_{jl}, calculated in Sec. III A 1. Since the expressions are bulky, we do not present them here, but discuss how this might be accomplished. The dependence on the Prandtl number is quite simple, and we explicitly consider it in the remaining part of this subsection.

For $\mathbf{k}=(k_1,k_2)=(k\cos\beta, k\sin\beta)$, $j=1,2,3$, denote by $\mathbf{g}_j(\mathbf{k},\gamma)$ the vector fields $\mathbf{f}_j(k,\gamma)$ [Eq. (17)] rotated by angle β about the vertical axis. Let $G(\mathbf{k},\gamma)$ be the subspace spanned by $\mathbf{g}_j(\mathbf{k},\gamma)$, $j=1,2,3$. By virtue of Eqs. (13) and (21),

$$N^{\mathrm{rc}}(\mathbf{X}_1,\mathbf{X}_2) = \sum_{s,l,j=1}^{3,8,8} C_{slj}^{+}\mathbf{g}_s(\mathbf{m}_1+\mathbf{m}_2, \gamma_l+\gamma_j) + \sum_{s,l,j=1}^{3,8,8} C_{slj}^{-}\mathbf{g}_s(\mathbf{m}_1-\mathbf{m}_2, \gamma_l+\gamma_j), \tag{69}$$

where $\mathbf{m}_1=(k_c,0)$ and $\mathbf{m}_2=k_c(\sin\alpha, \cos\alpha)$. Coefficients $C_{slj}^{\pm}$ can be easily calculated using Eqs. (13) and (21); they are independent of P.

For each pair $(\mathbf{k},\gamma)$, the subspace $G(\mathbf{k},\gamma)$ is L^{rc} invariant, and the 3×3 matrix [Eq. (18)] of L^{rc} acting in $G(\mathbf{k},\gamma)$ can be easily inverted numerically. The operator L^{rc} involves multiplication by P:

$$L^{\mathrm{rc}}(c_1\mathbf{g}_1 + c_2\mathbf{g}_2 + c_3\mathbf{g}_3) = Pd_1\mathbf{g}_1 + Pd_2\mathbf{g}_2 + d_3\mathbf{g}_3,$$

where c_j and d_j, $j=1,2,3$ do not depend on P. Hence, a solution to Eq. (67) is $\eta_1=\eta_{10}+P^{-1}\eta_{11}$ with η_{10} and η_{11} independent of P. The solution to Eq. (68) [which is identical to Eq. (15)] has been calculated in Sec. III A 1.

η_2 inherits the dependence on P from η_1 ($\eta_2=\eta_{20}+P^{-1}\eta_{21}$), and hence

$$\xi_{12}^1 = \xi_{12,0}^1 + P^{-1}\xi_{12,1}^1. \tag{70}$$

Note that $\xi_{12,m}^1$, $m=0,1$ can be calculated exactly and involve a finite number of terms.

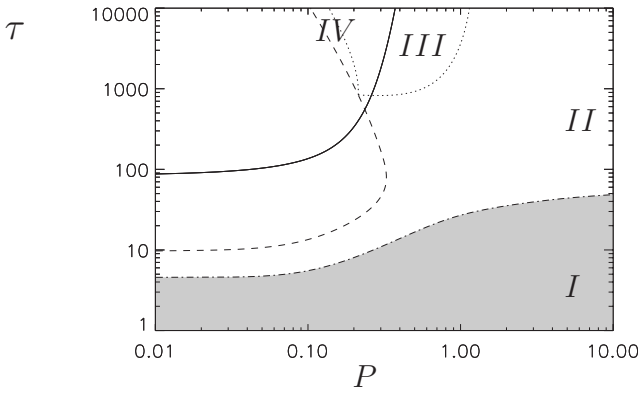

FIG. 7. The bifurcation diagram on the (P,τ) plane for the onset of nonmagnetic rotating convection. Solid line: the boundary between the steady and oscillatory onset of convection. Dashed line: the curve $a=0$ separating the regions of the subcritical and supercritical bifurcations of rolls. Dash-dotted line: the boundary of the region of stable rolls $\max_\alpha \min[b_1(\alpha)-a, b_2(\alpha)-a]=0$ for the supercritical bifurcation. Dotted lines: the boundaries of the regions of behavior of types II–IV for rolls bifurcating supercritically. The region where the rolls are stable is shaded.

The normal form coefficients are derived from the CM coefficients,

$$a = 2\mathrm{P}_{\mathbf{X}_1}[N(\mathbf{X}_1,\xi_{11})],$$

$$b_1 = 2\mathrm{P}_{\mathbf{X}_1}[N(\mathbf{X}_1,\xi_{22}) + 2N(\mathbf{X}_2,\xi_{12})],$$

$$b_2 = 2\mathrm{P}_{\mathbf{X}_2}[N(\mathbf{X}_2,\xi_{11}) + 2N(\mathbf{X}_1,\xi_{12})], \tag{71}$$

where $\mathrm{P}_{\mathbf{X}_i}$ is the projection onto $\mathbf{X}_i$,

$$\mathrm{P}_{\mathbf{X}_i}\mathbf{U} = (\mathbf{U}\cdot\mathbf{X}_i^*)(\mathbf{X}_i\cdot\mathbf{X}_i^*)^{-1}. \tag{72}$$

By virtue of Eqs. (64), (70), and (71) and since $\mathbf{X}_i$ do not depend on P, the normal form coefficients depend on the Prandtl number as follows:

$$a = \frac{a_0 + a_1P + a_2P^2}{P(c_0+c_1P)}, \tag{73}$$

$$b_j = \frac{b_{j0} + b_{j1}P + b_{j2}P^2}{P(c_0+c_1P)}, \quad j=1,2, \tag{74}$$

where a_s and c_s are functions of τ and b_{js} are functions of τ and α ($s=0,1,2$).

We have applied the simplest strategy to find the boundaries, on the (P,τ) plane, of the regions of the types of behavior I–IV: using the expressions that we derived, we have computed the coefficients $a_s(\tau)$, $b_{js}(\tau,\alpha)$ and $c_s(\tau)$ ($j=1,2$, $s=0,1,2$) for $1\le\tau\le10\,000$ and τ increased by factor $10^{0.004}$ at each step, and for $0<\alpha\le\pi/2$ step $\pi/500$, and analyzed the values a and b_j on this nonuniform grid.

2. Numerical results

The region where stable rolls emerge at the onset of convection is shown in Fig. 7 (shaded). Note that the line $a=0$

separating the regions of subcritical and supercritical bifurcations of rolls disagrees with the results of Clune and Knobloch [2], but agrees with the ones of Ahlers and Bajaj [23], Bodenschatz *et al.* [21], and Bajaj *et al.* [11]. (In [2] the bifurcation of rolls is subcritical if $P<1.1$ for some τ, while in our study and the other cited papers a subcritical bifurcation occurs only for $P<0.33$.)

As discussed in Sec. IV B, if rolls bifurcate supercritically, the regions of four types of behavior can be identified; the boundaries of the regions are described relations (59)–(62) for the normal form coefficients. The respective regions are labeled I–IV on Fig. 7. In region I, rolls are stable. In region II, "domain chaos" typical for Küppers-Lortz instability is observed, i.e., the convective regime is a sequence of events, in which patches of rolls are replaced by rolls rotated by a finite angle. In region III two types of behavior, different from the "domain chaos," are possible: there exist stable steady states which are (predominantly) sums of two roll patterns (e.g., squares), or such a rhombic pattern is observed in the temporal evolution intermittently with rolls. (We cannot distinguish the regions of these subtypes of behavior on the basis of our analysis.) In area IV, there exists a small perturbation of the trivial steady state increasing (in the linear and the subsequent nonlinear evolution) to infinity, and hence at the onset finite-amplitude flows can be observed.

The regions, where the nonlinear behavior is of types III and IV (i.e., rolls bifurcate supercritically and they are unstable, but the instability is not of the Küppers-Lortz type) are present in Fig. 7 for $\tau>800$. In region III, the angle α between the rolls comprising the potentially stable steady state $S_3(\alpha)$ is within the interval $\beta\le\alpha\le\pi/2$, with β close to $\pi/2$; thus, stable squares are not ruled out. Interestingly, stable squares were unexpectedly observed in experiments close to the onset of convection, which is not yet explained [17,21,23]. They were reported for $P=0.69$ and $P\sim 5$ for $140\le\tau\le 500$. Rhombic patterns and squares near the onset of convection in a rotating layer were observed in numerical simulations in [18] for $P=6.4$ and $\tau=548$. None of these values agree with Fig. 7. However, we consider only patterns of critical wave numbers, and for other wave numbers the boundaries between different types of instabilities are shifted. Thus, type IIIa instability of rolls can, in principle, furnish an explanation of emergence of stable rhombs and squares in experiments (but note the discussion at the end of Sec. IV B).

D. Convection with magnetic field, no rotation

1. Calculation of coefficients in Eq. (56)

We proceed here as in Sec. IV C. The operator L^{mc} [Eq. (7) with $\tau=0$] acts in the space $\mathcal{H}^{\mathrm{mc}}_{\alpha}$ of seven-component vector fields [Eq. (6)], periodic on the rhombic lattice with an acute angle α and satisfying the boundary conditions [Eqs. (9) and (10)]. At the steady-state bifurcation of $\mathbf{w}=0$, the operator possesses a four-dimensional kernel, the center eigenspace is comprised of $\mathbf{X}_1$ calculated in Sec. III B 1, and $\mathbf{X}_2$ and $\mathbf{Y}_j$, $j=1,2$ obtained from $\mathbf{X}_1$ as in Sec. IV C. The center manifold is sought in the form Eq. (63), its coefficients are calculated from

$$L^{\mathrm{mc}}\xi^1_{11}+N(\mathbf{X}_1,\mathbf{X}_1)=0,\quad L^{\mathrm{mc}}\xi^1_{12}+2N(\mathbf{X}_1,\mathbf{X}_2)=0. \tag{75}$$

As an example, we solve here the second equation in Eq. (75). The CM coefficient ξ^1_{12} is assumed in the form Eq. (66), η_1 and η_2 can be found from the equations similar to Eqs. (67) and (68) (where we replace $L^{\mathrm{rc}}\to L^{\mathrm{mc}}$ and $N^{\mathrm{rc}}\to N$). For $\mathbf{k}=(k_1,k_2)=(k\cos\beta, k\sin\beta)$, denote by $\mathbf{g}_j(\mathbf{k},\gamma)$, $j=1,3,4$, the vector fields $\mathbf{f}_j(k,\gamma)$ (defined in Sec. III B) rotated by the angle β about the vertical axis. Due to Eq. (38), the nonlinear term is a sum of the form

$$N(\mathbf{X}_1,\mathbf{X}_2)=\sum_{s=1,3,4}\sum_{l,j=1}^{8,8} C^{\pm}_{slj}\mathbf{g}_s(\mathbf{m}_1\pm\mathbf{m}_2,\gamma_l+\gamma_j),$$

$$C^{\pm}_{1lj}=c^{\pm}_{1lj1}+Pqc^{\pm}_{1lj2},\quad C^{\pm}_{3lj}=c^{\pm}_{3lj1},\quad C^{\pm}_{4lj}=c^{\pm}_{4lj1}+qc^{\pm}_{4lj2}, \tag{76}$$

where $\mathbf{m}_1=(k_c,0)$, $\mathbf{m}_2=k_c(\sin\alpha,\cos\alpha)$ and $c^{\pm}_{sljm}$ are independent of P and q. The coefficients can be calculated using Eqs. (8) and (38).

For each pair $(\mathbf{k},\gamma)$, the subspace $G(\mathbf{k},\gamma)$ spanned by $\mathbf{g}_1(\mathbf{k},\gamma)$, $\mathbf{g}_3(\mathbf{k},\gamma)$ and $\mathbf{g}_4(\mathbf{k},\gamma)$ is L^{mc} invariant; the action of L^{mc} in $G(\mathbf{k},\gamma)$ is described by the 3×3 matrix [Eq. (35)]. Like in Sec. IV C, we will trace the dependence of the relevant quantities on P and q. The operator L^{mc} involves multiplication by P and division by q,

$$L^{\mathrm{mc}}(c_1\mathbf{g}_1+c_3\mathbf{g}_3+qc_4\mathbf{g}_4)=Pd_1\mathbf{g}_1+Pd_3\mathbf{g}_3+d_4\mathbf{g}_4,$$

where c_j and d_j, $j=1,2,3$, do not depend on P and q. Hence, the solution to Eq. (65) is sought in the following form:

$$\eta^1_{12}=\sum_{s=1,3,4}\sum_{j=1}^{J} D^{\pm}_{sj}\mathbf{g}_s(\mathbf{m}_1\pm\mathbf{m}_2,\gamma_j),$$

where

$$D^{\pm}_{1j}=d^{\pm}_{1j1}+P^{-1}d^{\pm}_{1j2}+qd^{\pm}_{1j3},\quad D^{\pm}_{3j}=d^{\pm}_{3j1}+P^{-1}d^{\pm}_{3j2}+qd^{\pm}_{3j3},$$

$$D^{\pm}_{4j}=qd^{\pm}_{4j1}+qP^{-1}d^{\pm}_{4j2}+q^2d^{\pm}_{4j3}, \tag{77}$$

$J=72$ (because 8×8 terms are involved in η_1 and 8 in η_2), $\mathbf{m}_1=(k_c,0)$, $\mathbf{m}_2=k_c(\sin\alpha,\cos\alpha)$. $d^{\pm}_{sjm}$ are independent of P and q.

The operator $L^{\mathrm{mc},*}$ adjoint to L^{mc} for the scalar product

$$\mathbf{w}_1\cdot\mathbf{w}_2=\mathbf{v}_1\cdot\mathbf{v}_2+PR\theta_1\cdot\theta_2+Pq^{-1}\mathbf{b}_1\cdot\mathbf{b}_2 \tag{78}$$

and the dual basis X^*_j and Y^*_j, $j=1,2$, are obtained from L^{mc} and X_j and Y_j by inversion of the sign of Q. By virtue of Eqs. (72), (77), and (78), the coefficients of the normal form Eq. (56) depend on P and q as follows:

$$a=\frac{a_0+a_1P+a_2Pq+a_3P^2+a_4P^2q+a_5P^2q^2}{P(c_0+c_1P+c_2Pq)}, \tag{79}$$

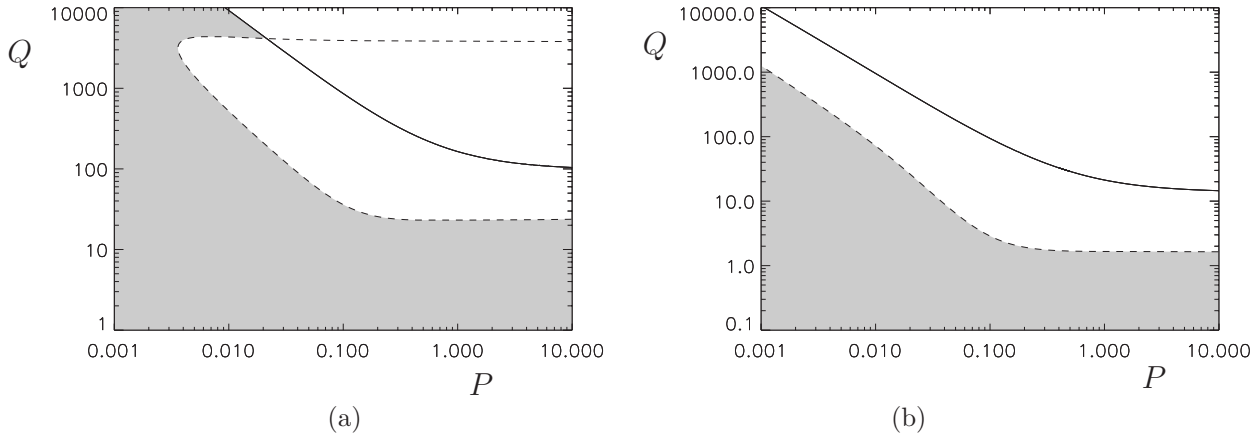

FIG. 8. The bifurcation diagram on the (P,Q) plane for the onset of magnetoconvection, (a) $q=3$, and (b) $q=10$. Lines of different types represent boundaries of the same kind as in Fig. 7.

$$b_j = \frac{b_{j0} + b_{j1}P + b_{j2}Pq + b_{j3}P^2 + b_{j4}P^2q + b_{j5}P^2q^2}{P(c_0 + c_1P + c_2Pq)}, \quad j = 1,2. \tag{80}$$

Here a_s and c_s are functions of Q, and b_{js} are functions of Q and $\alpha(s=0,\ldots,5)$.

2. Numerical results

The regions on the (P,Q) and (q,Q) planes where magnetoconvection sets in as stable rolls are shown in Figs. 8 and 9. Rolls are stable, if $q<1$ or if Q or P are sufficiently small, and for $q \gg 1$ and large values of any of two other parameters they are unstable. The regions of stable rolls are bounded by the curves $a=0$ (i.e., the boundary between the subcritical and supercritical bifurcations of rolls) and the boundary between the monotonic and oscillatory instability. This is in contrast with nonmagnetic rotating convection, where the region of stability is bounded by the boundary of the Küppers-Lortz instability, the curve $\max_\alpha \max[b_1(\alpha) - a, b_2(\alpha) - a] = 0$.

E. Rotating convection with magnetic field

1. Calculation of coefficients in Eq. (56)

Proceeding as in Secs. IV C and IV D, we consider the operator L [Eq. (7)] acting on the space $\mathcal{H}_\alpha$ of seven-component vector fields [Eq. (6)], periodic on the rhombic lattice with an acute angle α and satisfying boundary conditions [Eqs. (9) and (10)]. The center eigenspace is spanned by $\mathbf{X}_1$ found in Sec. III C 1 and $\mathbf{X}_2$, $\mathbf{Y}_j$, $j=1,2$ obtained from $\mathbf{X}_1$ as in Secs. IV C and IV D. Coefficients of the center manifold [Eq. (63)] are calculated from [Eq. (65)] (where L and N instead of L^{rc} and N^{rc}, respectively, are assumed).

Like in the previous subsection, considering the mapping N [Eq. (8)] and the action of L [Eq. (49)] on $G(\mathbf{k},\gamma)$ spanned by $\mathbf{g}_j(\mathbf{k},\gamma)$, $j=1,\ldots,5$, we find that the dependence of a, b_1 and b_2 on P and q is determined by Eqs. (79) and (80), where a_s and c_s are functions of Q and τ, and b_{js} are functions of Q, τ, and $\alpha(s=0,\ldots,5)$.

2. Numerical results

The regions on the (P,τ) plane where rolls are stable at the onset of convection are shaded in gray in Figs. 10 and 11 for several values of Q and q. The regions have a different

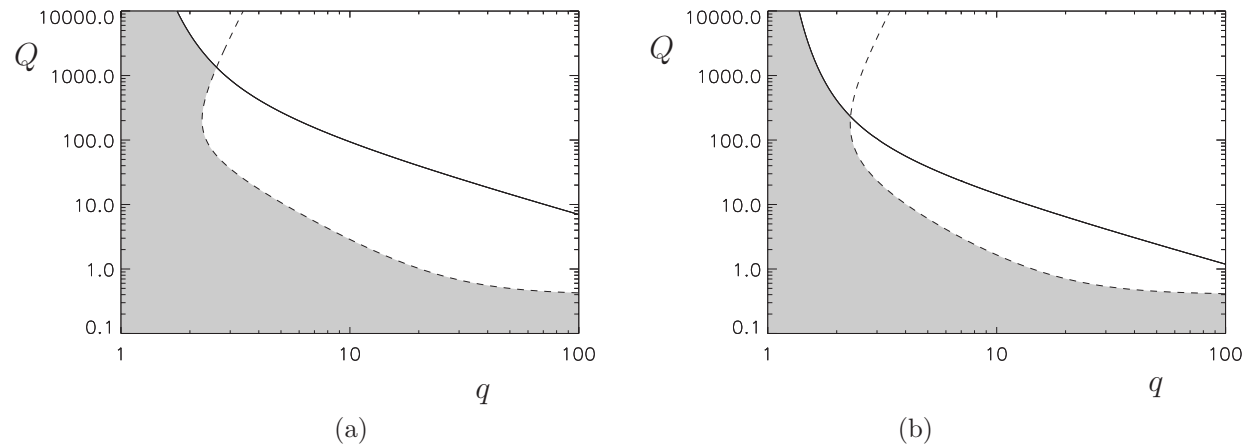

FIG. 9. The bifurcation diagram on the (q,Q) plane for the onset of magnetoconvection. (a) $P=0.1$ and (b) $P=10$. Lines of different types represent boundaries of the same kind as in Fig. 7.

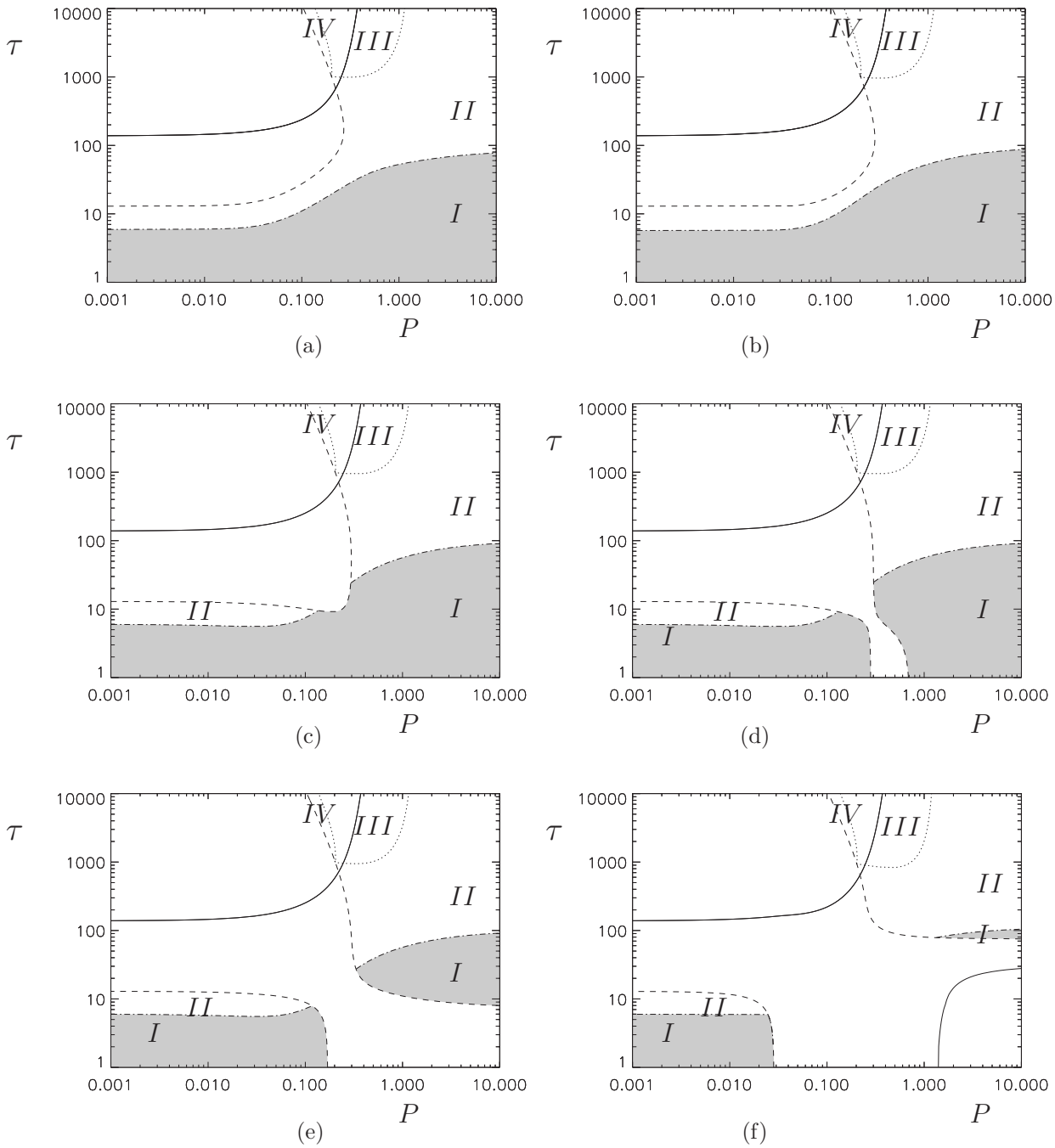

FIG. 10. The bifurcation diagram on the (P,τ) plane for the onset of rotating magnetoconvection for $Q=50$ and (a) $q=0.01$, (b) $q=2$, (c) $q=2.5$, (d) $q=2.51$, (e) $q=2.55$, (f) $q=5$. Lines of different types represent boundaries of the same kind as in Fig. 7.

shape for $q\leq 1$ and $q>1$. For $q\leq 1$ (similarly to nonmagnetic rotating convection) the region of stable rolls is bounded only from above by the line $\max_\alpha[b_1(\alpha)-a,b_2(\alpha)-a]=0$, and for sufficiently small τ rolls are stable for all P. The boundary of stable rolls moves up when Q increases. Experiments and the interior of the Earth are characterized by the values $q<1$, which are therefore of special interest. We have investigated numerically the dependence of the critical angle α_c on P for some Q and $q\leq 1$ (see Fig. 12). For small P, α_c decreases with Q, possibly vanishing for $Q\to\infty$. For large P, α_c remains close to the critical value of rotating convection.

For $q>1$ the shape of the region significantly varies with q. The middle parts $(P\sim 1)$ of the lines $a=0$ and $\max_\alpha \max[b_1(\alpha)-a,b_2(\alpha)-a]=0$ bounding the regions of stable rolls move down as q increases. As a result, two disconnected components of the region of stable rolls at the onset emerge for sufficiently large q: stable rolls exist either for small P and τ or for large P and small and moderate values of τ.

Only a few experiments on rotating magnetoconvection were carried out. Experiments by Nakagawa [24] and more recent ones by Aurnou and Olson [7] were focused on investigation of the competition between the steady and oscilla-

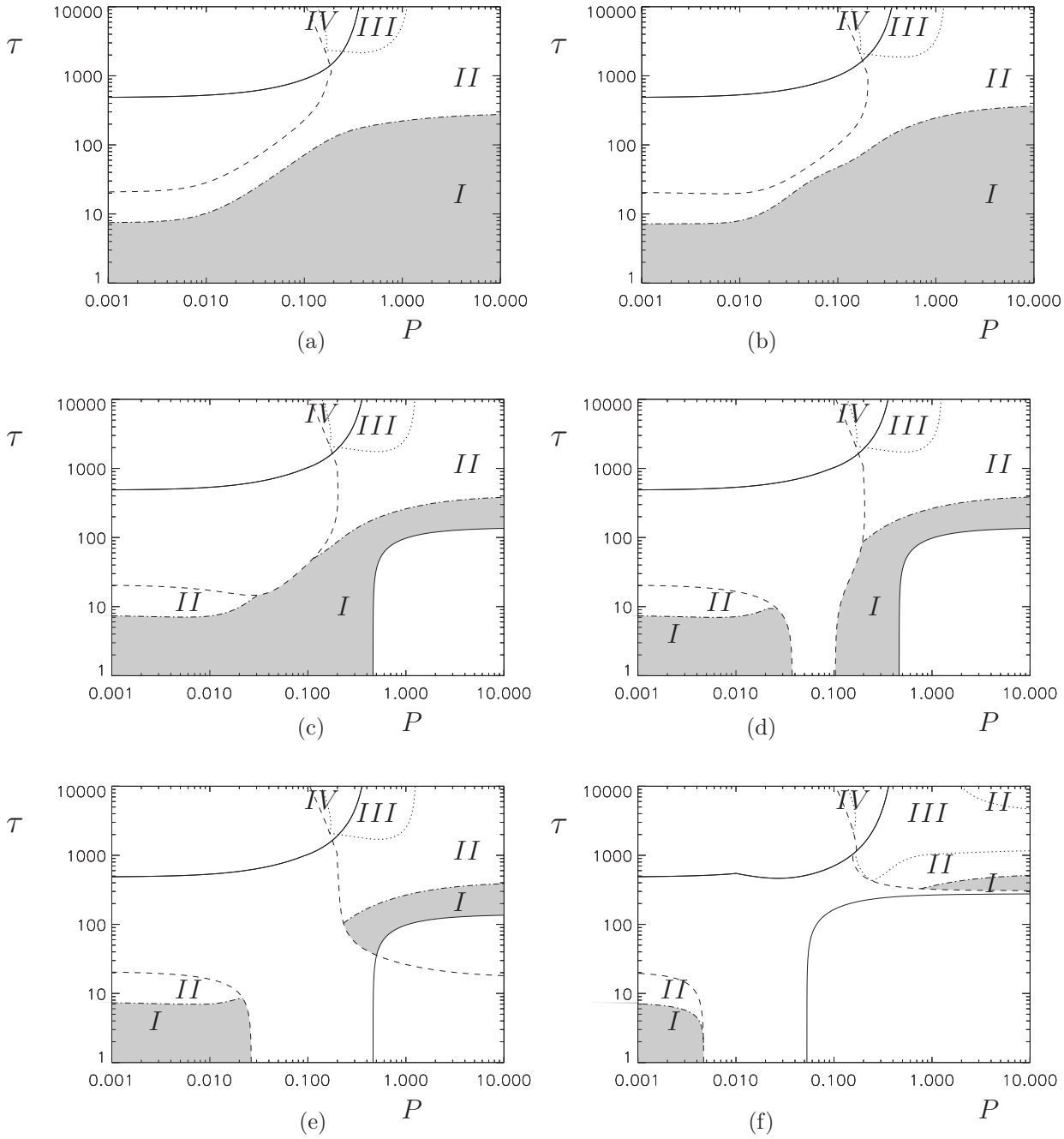

FIG. 11. The bifurcation diagram on the (P,τ) plane for the onset of rotating magnetoconvection for $Q=500$ and (a) $q=0.01$, (b) $q=2$, (c) $q=2.3$, (d) $q=2.36$, (e) $q=2.4$, and (f) $q=5$. Lines of different types represent boundaries of the same kind as in Fig. 7.

tory onset of convection, nonlinear regimes of convection near the onset and dependence of the Nusselt number on the Rayleigh number. The experimental results on linear stability agree reasonably well with the theory (see discussion in Zhang *et al.* [6]). The stationary onset of convection was observed only exceptionally by Aurnou and Olson (for the strongest employed magnetic field and the smallest aspect ratio); this also conforms with our findings that rolls are unstable for the parameter values for which the experiments were conducted, and that on increasing strength of the imposed magnetic field the region of stable rolls grows.

V. CONCLUSION

We have considered the onset of convection in a horizontal layer of conducting fluid rotating about a vertical axis with an imposed vertical magnetic field. The first instability of fluid at rest is steady or oscillatory, depending on parameters of the problem. Oscillatory instability occurs for small P, providing the Taylor number is sufficiently large, or for large P and Q if $q>1$ (where q is the Roberts number). For large Q and q, two regions on the (P,τ) plane of the oscillatory onset of convection merge, creating thus two regions of the steady onset of convection.

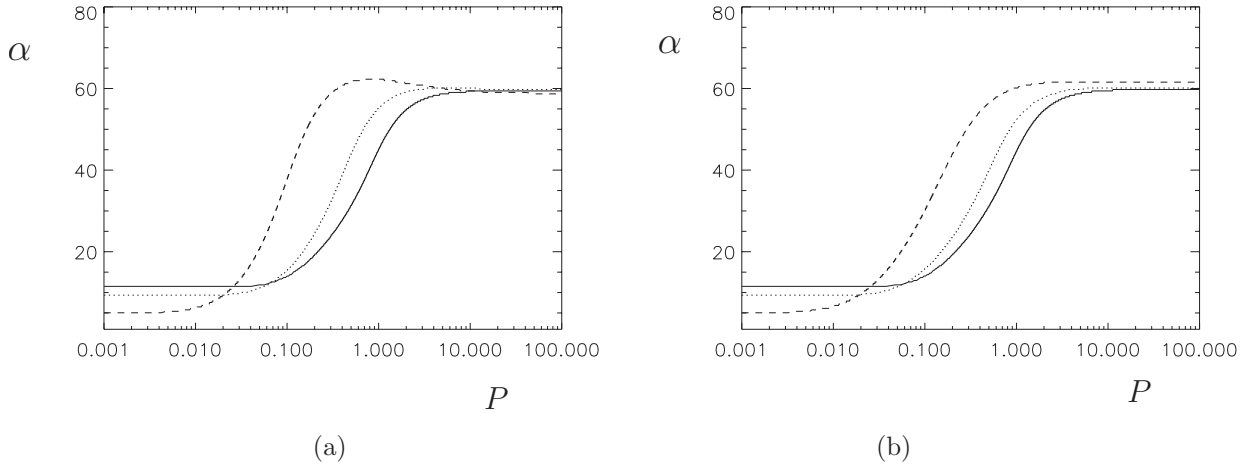

FIG. 12. The critical angle α_c for instability of rolls in rotating magnetoconvection as a function of P for (a) $q=1$ and (b) $q=0.01$ for $Q=5$, 50 and 500 (solid, dotted, and dashed lines, respectively).

We have shown that if rolls bifurcate supercritically and are unstable near the onset, two types of weakly nonlinear behavior of perturbations are possible in addition to the Küppers-Lortz instability. In rotating nonmagnetic convection, stable squares observed in experiments are apparently related to this instability.

Stability of rolls at the onset of convection in a nonrotating layer with an imposed magnetic field that we have considered was not studied for the physical boundary conditions before. Rolls are unstable at the onset of magnetoconvection, if Q, q, or P are sufficiently large. For two parameters fixed, rolls are stable if the third one is small enough.

In rotating magnetoconvection for $q<1$, stable rolls are observed for all P, if τ is not large. For $q>1$, dependence of the region of stability on other parameters is more complex, in particular, two disconnected regions, in which rolls are observed at the onset of convection, can be present on the (P,τ) plane.

Note that stability of rolls with the critical wave number only was examined. It is well known (see, e.g., [10,25,26]) that rolls with other wave numbers have different stability properties. To examine how stability of rolls depends on the wave number is an important open problem that we leave for the future investigation.

ACKNOWLEDGMENTS

A part of this research was carried out during my visit to the School of Engineering, Computer Science and Mathematics, University of Exeter, U.K. I am grateful to the Royal Society for their financial support. My research visits to Observatoire de la Côte d'Azur were supported by the French Ministry of Education. I was partially supported by the Grant No. ANR-07-BLAN-0235 OTARIE from Agence nationale de la recherche, France, and by the Grant No. 07-01-92217-CNRSL_a from the Russian foundation for basic research. I thank Dr. J. H. P. Dawes for bringing to my attention the Refs. [23,27]. Last but not least, I thank an anonymous referee for valuable remarks.

APPENDIX: PREDICTIONS FROM BIFURCATION THEORY

In this appendix we explore possible generic types of behavior of solutions to a system of the form

$$\dot{x} = (\lambda + B_1 x^2 + B_2 y^2)x,$$

$$\dot{y} = (\mu + C_1 y^2 + C_2 x^2)y, \tag{A1}$$

assuming

$$\lambda > 0, \quad \mu > 0, \quad B_1 < 0, \quad C_1 < 0. \tag{A2}$$

B_2 and C_2 are arbitrary. The condition (A2) implies existence of steady states $S_1=(x_1,0)=(\pm\sqrt{-\lambda/B_1},0)$ and $S_2=(0,y_2)=(0,\pm\sqrt{-\mu/C_1})$, which are stable along the directions $(x,0)$ and $(0,y)$, respectively.

Lemma 1. The system [Eqs. (A1) and (A2)] does not admit periodic orbits.

Proof. Changing variables $x\to x^2$, $y\to y^2$, and $t\to t/2$, we transform Eq. (A1) into a two-dimensional Lotka-Volterra equation

$$\dot{x} = (\lambda + B_1 x + B_2 y)x,$$

$$\dot{y} = (\mu + C_1 y + C_2 x)y, \tag{A3}$$

which we consider in the quadrant $x\geq 0$, $y\geq 0$. By theorem 4.2.1 and Exercise 4.2.3 of Hofbauer and Sigmund [27], Eq. (A3) does not have isolated periodic orbits, and it has a continuum of periodic orbits, if

$$B_1 + C_1 = 0, \quad B_1(\lambda C_1 - \mu B_2) + C_1(\mu B_1 - \lambda C_2) = 0,$$

$$B_1 C_1 - B_2 C_2 < 0,$$

which is incompatible with Eq. (A2). The lemma is proved.

Theorem. The system [Eqs. (A1) and (A2)] can exhibit the following four generic types of behavior,

(i) If

$$\lambda - \frac{\mu B_2}{C_1} < 0, \quad \mu - \frac{\lambda C_2}{B_1} < 0, \tag{A4}$$

then the steady states S_1 and S_2 are stable, there exist an unstable steady state $S_3=(x_3,y_3)$, $x_3y_3\neq 0$, and heteroclinic connections from S_3 to S_1 and S_2.

(ii) If

$$\lambda - \frac{\mu B_2}{C_1} < 0, \quad \mu - \frac{\lambda C_2}{B_1} > 0, \tag{A5}$$

then the only steady states of the system are $S_0=(0,0)$, S_1 and S_2; S_1 is unstable and S_2 is stable, and there exists a heteroclinic connection from S_1 to S_2.

(ii′) If

$$\lambda - \frac{\mu B_2}{C_1} > 0, \quad \mu - \frac{\lambda C_2}{B_1} < 0, \tag{A6}$$

then the only steady states of the system are $S_0=(0,0)$, S_1 and S_2; S_1 is stable and S_2 is unstable, and there exists a heteroclinic connection from S_2 to S_1.

(iii) If

$$\lambda - \frac{\mu B_2}{C_1} > 0, \quad \mu - \frac{\lambda C_2}{B_1} > 0, \quad B_1C_1 - B_2C_2 > 0, \tag{A7}$$

then the steady states S_1 and S_2 are unstable, there exist a stable steady state $S_3=(x_3,y_3)$, $x_3y_3\neq 0$, and heteroclinic connections from S_1 and S_2 to S_3.

(iv) If

$$\lambda - \frac{\mu B_2}{C_1} > 0, \quad \mu - \frac{\lambda C_2}{B_1} > 0, \quad B_1C_1 - B_2C_2 < 0, \tag{A8}$$

then the only steady states of the system are $S_0=(0,0)$, S_1 and S_2, and all the three are unstable. Any trajectory $[x(x_0,y_0,t),y(x_0,y_0,t)]$ starting at any point (x_0,y_0), $x_0y_0\neq 0$, escapes to infinity, i.e.,

$$\lim_{t\to\infty} x(x_0,y_0,t) = \infty, \quad \lim_{t\to\infty} y(x_0,y_0,t) = \infty. \tag{A9}$$

Proof. (i) Assume Eq. (A4). Conditions (A2) and (A4) imply

$$\lambda C_1 - \mu B_2 > 0, \quad \mu B_1 - \lambda C_2 > 0, \quad C_1B_1 - B_2C_2 < 0, \tag{A10}$$

hence $S_3=(x_3,y_3)$, where

$$x_3^2 = \frac{\lambda C_1 - \mu B_2}{B_2C_2 - B_1C_1}, \quad y_3^2 = \frac{\mu B_1 - \lambda C_2}{B_2C_2 - B_1C_1}, \tag{A11}$$

is a steady state of Eq. (A1).

The matrix of linearization of Eq. (A3) near $\tilde{S}_3=(x_3^2,y_3^2)$, the respective steady state of Eq. (A3), is

$$\begin{pmatrix} B_1x_3^2 & B_2x_3^2 \\ C_2y_3^2 & C_1y_3^2 \end{pmatrix}. \tag{A12}$$

By virtue of Eq. (A10), its determinant

$$x_3^2y_3^2(B_1C_1 - B_2C_2) \tag{A13}$$

is negative, implying that Eq. (A12) possesses two real eigenvalues of different signs. Thus, $\tilde{S}_3$ and S_3 are unstable steady states of the respective systems. By virtue of Eqs. (A2) and (A4), all entries of the matrix [Eq. (A12)] are negative, and hence the unstable eigendirections for S_3 and $\tilde{S}_3$ are of the form $(1,-h)$, $h>0$.

Consider Eq. (A1) in a rectangle $[x_3,\bar{x}]\times[0,y_3]$ for $\bar{x}>x_1$. On the side $x=x_3$, $\dot{x}\geq 0$, because $\dot{x}$ is a product of a linear function of y^2, non-negative at both end points, (x_3,y_3) and $(x_3,0)$, and of $x\geq 0$. Similarly, $\dot{x}\leq 0$ on the side $x=\bar{x}$ and $\dot{y}\leq 0$ on the side $y=y_3$; $\dot{y}=0$ for $y=0$. Thus, no trajectories escape from the rectangle. An unstable half-manifold of S_3 stretches into the rectangle, and in the limit $t\to\infty$ it has no other choice but to approach S_1. Existence of a connection from S_3 to S_1 is proved. Existence of a connection from S_3 to S_2 can be demonstrated similarly.

(ii) Assume Eq. (A5). Conditions (A2) and (A5) imply

$$\lambda C_1 - \mu B_2 > 0, \quad \mu B_1 - \lambda C_2 < 0, \tag{A14}$$

and hence no (x_3,y_3) can satisfy Eq. (A11).

Consider Eq. (A1) in a rectangle $[0,\bar{x}]\times[0,\bar{y}]$, where $\bar{y}>y_2$ and $\bar{x}>\max(x_1,-(\lambda+B_2\bar{y}^2)/B_1)$. The derivatives $\dot{x}$ and $\dot{y}$ are negative on the sides $x=\bar{x}$ and $y=\bar{y}$, respectively, like in case (i). Therefore, no trajectories escape from the rectangle, and hence the unstable manifold of S_1 approaches S_2. Existence of a heteroclinic connection is proved.

(ii′) The proof is identical to the proof of *ii* with the variables x and y interchanged.

(iii) Assume Eq. (A7). By virtue of Eqs. (A2) and (A7),

$$\lambda C_1 - \mu B_2 < 0, \quad \mu B_1 - \lambda C_2 < 0, \quad B_1C_1 - B_2C_2 > 0 \tag{A15}$$

implying existence of a steady state [Eq. (A11)]. Due to Eq. (A7), the determinant [Eq. (A13)] of the matrix [Eq. (A12)] is positive, and due to Eq. (A2) its trace is negative. Thus, the matrix has either two real negative eigenvalues or a pair of complex eigenvalues with negative real parts, and thus the steady state S_3 is stable.

Suppose

$$C > \max\left(1, -\frac{\lambda}{B_1x_3^2}, -\frac{\mu}{C_1y_3^2}\right), \quad (\bar{x},\bar{y}) = C^{1/2}(x_3,y_3).$$

Consider the rectangle $[0,\bar{x}]\times[0,\bar{y}]$. The derivatives $\dot{x}$ and $\dot{y}$ in Eq. (A1) are negative on the sides $x=\bar{x}$ and $y=\bar{y}$, respectively, like in case (i). Thus, trajectories do not escape from the rectangle. Conditions (A7) imply that S_1 and S_2 are unstable. Inside the rectangle, the only stable steady state is S_3. By lemma 1, there are no periodic orbits. Hence, unstable manifolds of S_1 and S_2 are attracted by S_3.

(iv) Assume Eq. (A8) and consider the system [Eq. (A3)]. Conditions (A2) and (A8) imply

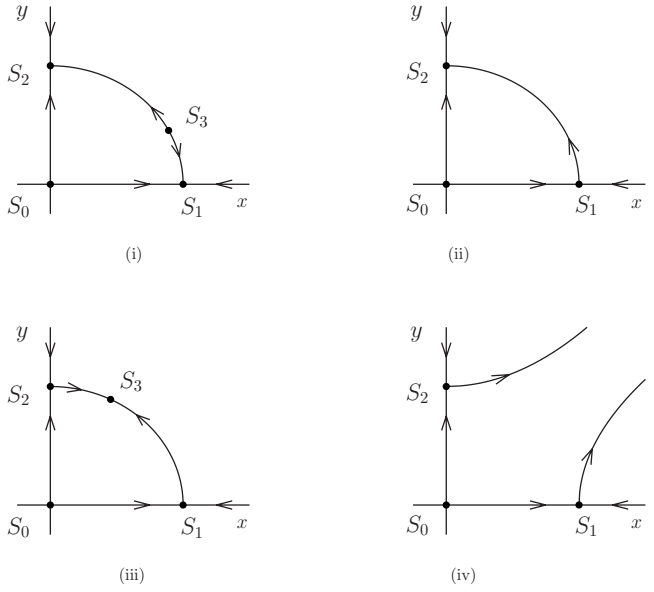

FIG. 13. Sketches of phase portraits of the system [Eq. (A1)] in the cases (i)–(iv).

$$C_1\lambda - \mu B_2 < 0, \quad B_1\mu - \lambda C_2 < 0, \quad B_1C_1 - B_2C_2 < 0, \tag{A16}$$

and therefore the values [Eq. (A11)] are negative. Hence S_0, S_1 and S_2 are the only steady states. Let $\epsilon > 0$ be a small number such that

$$\epsilon < \min\left(-\frac{\lambda}{B_1}, -\frac{\mu}{C_1}\right). \tag{A17}$$

Denote

$$\mathbf{R}^2_\epsilon = \{(x,y): x > \epsilon, y > \epsilon\}.$$

The lines $\lambda + B_1x + B_2y - s\epsilon = 0$ and $\mu + C_1y + C_2x - d\epsilon = 0$, where

$$0 < s < \min\left(\frac{\lambda}{\epsilon}, \frac{B_1}{B_1C_1 - B_2C_2}\right), \quad 0 < d < \min\left(\frac{\mu}{\epsilon}, \frac{C_1}{B_1C_1 - B_2C_2}\right), \tag{A18}$$

divide the region $\mathbf{R}^2_\epsilon$ into three parts,

$$\mathbf{R}^2_{\epsilon,I} = \left\{(x,y): x > \epsilon, y > -\frac{C_2x + \mu - d\epsilon}{C_1}\right\},$$

$$\mathbf{R}^2_{\epsilon,II} = \left\{(x,y): x > \epsilon, \ \max\left(\epsilon, -\frac{\lambda + B_1x - s\epsilon}{B_2}\right) < y < -\frac{C_2x + \mu - d\epsilon}{C_1}\right\},$$

$$\mathbf{R}^2_{\epsilon,III} = \left\{(x,y): y > \epsilon, \ x > -\frac{B_2y + \lambda - s\epsilon}{B_1}\right\}.$$

In $\mathbf{R}^2_{\epsilon,II}$ the derivatives $\dot{x}$ and $\dot{y}$ in Eq. (A3) are bounded from below,

$$\dot{x} = x(\lambda + B_1x + B_2y) > xs\epsilon > s\epsilon^2, \quad \dot{y} = y(\mu + C_1y + C_2x) > yd\epsilon > d\epsilon^2. \tag{A19}$$

If d satisfies Eq. (A18), then $\dot{x}/\dot{y} > -C_1/C_2$ on the line $\mu + C_1y + C_2x - d\epsilon = 0$, and hence trajectories can pass from $\mathbf{R}^2_{\epsilon,I}$ to $\mathbf{R}^2_{\epsilon,II}$, but not in the opposite direction. Similarly, no trajectories leave from $\mathbf{R}^2_{\epsilon,II}$ to $\mathbf{R}^2_{\epsilon,III}$. Therefore, any trajectory starting in $\mathbf{R}^2_{\epsilon,II}$ remains there, which due to Eq. (A19) implies Eq. (A9) for any $(x_0,y_0) \in \mathbf{R}^2_{\epsilon,II}$.

In $\mathbf{R}^2_{\epsilon,I}$, $\dot{x}$ is bounded from below [see Eq. (A19)]. Any trajectory starting at $(x_0,y_0) \in \mathbf{R}^2_{\epsilon,I}$ either enters $\mathbf{R}^2_{\epsilon,II}$, which implies [Eq. (A9)], or it stays in $\mathbf{R}^2_{\epsilon,I}$. In the latter case $\lim_{t\to\infty} x(x_0,y_0,t) = \infty$ due to Eq. (A19). Since the trajectory never crosses the line $\mu + C_1y + C_2x - d\epsilon = 0$, $\lim_{t\to\infty} y(x_0,y_0,t) = \infty$. Equation (A9) holds for any $(x_0,y_0) \in \mathbf{R}^2_{\epsilon,I}$. Similarly, Eq. (A9) holds true for any $(x_0,y_0) \in \mathbf{R}^2_{\epsilon,III}$. The theorem is proved. Sketches of phase portraits of the system [Eq. (A1)] are shown in Fig. 13.

[1] S. Chandrasekhar, *Hydrodynamic and Hydromagnetic Stability* (Clarendon Press, Oxford, 1961).
[2] T. Clune and E. Knobloch, Phys. Rev. E **47**, 2536 (1993).
[3] M. Weeks and K. Zhang, Geophys. Astrophys. Fluid Dyn. **96**, 405 (2002).
[4] P. Roberts and K. Zhang, J. Fluid Mech. **420**, 201 (2000).
[5] I. A. Eltayeb, Proc. R. Soc. London, Ser. A **326**, 229 (1972); J. Fluid Mech. **71**, 161 (1975).
[6] K. Zhang, M. Weeks, and P. Roberts, Phys. Fluids **16**, 2023 (2004).
[7] J. M. Aurnou and P. L. Olson, J. Fluid Mech. **430**, 283 (2001).
[8] O. Podvigina, Mekhanika zhidkosti i gaza **4**, 29 (2009) (in Russian) Fluid Dyn. [English translation, **44**, 502 (2009)].
[9] G. Küppers and D. Lortz, J. Fluid Mech. **35**, 609 (1969).
[10] R. M. Clever and F. H. Busse, J. Fluid Mech. **94**, 609 (1979).
[11] K. M. S. Bajaj, G. Ahlers, and W. Pesch, Phys. Rev. E **65**, 056309 (2002).
[12] D. Lortz, J. Fluid Mech. **23**, 113 (1965).
[13] T. Clune and E. Knobloch, Physica D **74**, 151 (1994).
[14] M. R. E. Proctor, in *Fluid Dynamics and Dynamos in Astrophysics and Geophysics*, edited by A. M. Soward, C. A. Jones, D. W. Hughes, and N. O. Weiss (CRC Press, Boca Raton, FL, 2005).
[15] A. Pellew and R. V. Southwell, Proc. R. Soc. London, Ser. A **176**, 312 (1940).
[16] F. Zhong, R. E. Ecke, and V. Steinberg, Phys. Rev. Lett. **67**, 2473 (1991); H. F. Goldstein, E. Knobloch, I. Mercader, and M. Net, J. Fluid Mech. **248**, 583 (1993).

[17] K. M. S. Bajaj, J. Liu, B. Naberhuis, and G. Ahlers, Phys. Rev. Lett. **81**, 806 (1998).
[18] J. J. Sánchez-Álvarez, E. Serre, E. Crespo del Arco, and F. H. Busse, Phys. Rev. E **72**, 036307 (2005).
[19] J. J. Sánchez-Álvares, E. Crespo del Arco, and F. H. Busse, J. Fluid Mech. **600**, 427 (2008).
[20] W. H. Press, B. P. Flannery, S. A. Teukolsky, and W. T. Vetterling, *Numerical Recipes in Fortran: The Art of Scientific Computing* (CUP, Cambridge, 1992), Vol. 1.
[21] E. Bodenschatz, W. Pesch, and G. Ahlers, Annu. Rev. Fluid Mech. **32**, 709 (2000).
[22] O. Podvigina, Dyn. Syst. **21**, 191 (2006).
[23] G. Ahlers and K. M. S. Bajaj, in *Pattern Formation in Continuous and Coupled Systems*, edited by M. Golubitsky, D. Luss, and S. H. Strogatz (Springer-Verlag, New York, 1999).
[24] Y. Nakagawa, Proc. R. Soc. London, Ser. A **242**, 81 (1957); **249**, 138 (1959).
[25] F. H. Busse and R. M. Clever, Arch. Mech. **43**, 565 (1991).
[26] O. Podvigina, Geophys. Astrophys. Fluid Dyn. **104**, 1 (2010).
[27] J. Hofbauer and K. Sigmund, *Evolutionary Games and Population Dynamics* (CUP, Cambridge, 1998).